

# Elevated-Temperature Metathesis Syntheses of Structurally Novel Alkali-Metal Tetrakis(3,5-di-*tert*-butylpyrazolato)lanthanoidate(III) Complexes: Toluene-Coordinated Discrete Bimetallic Complexes and Supramolecular Chains

Glen B. Deacon,<sup>\*,[a]</sup> Ewan E. Delbridge,<sup>[a]</sup> David J. Evans,<sup>[a]</sup> Rita Harika,<sup>[a]</sup> Peter C. Junk,<sup>\*,[a]</sup> Brian W. Skelton,<sup>[b]</sup> and Allan H. White<sup>[b]</sup>

**Abstract:** Sodium and potassium tetrakis(3,5-di-*tert*-butylpyrazolato)lanthanoidate(III) complexes  $[M\{Ln(tBu_2pz)_4\}]$  have been prepared by reaction of anhydrous lanthanoid trihalides with alkali metal 3,5-di-*tert*-butylpyrazolates at 200–300 °C, and a 1,2,4,5-tetramethylbenzene flux for  $M=K$ . On extraction with toluene (or occasionally directly from the reaction tube) the following complexes were isolated:  $[Na(PhMe)\{Ln(tBu_2pz)_4\}]$  (**1Ln**; **1Ln** = **1Tb**, **1Ho**, **1Er**, **1Yb**),  $[K(PhMe)\{Ln(tBu_2pz)_4\}] \cdot 2PhMe$  (**2Ln**; **2Ln** = **2La**, **2Sm**, **2Tb**, **2Ho**, **2Yb**, **2Lu**),  $[Na\{Ln(tBu_2pz)_4\}]_n$  (**3Ln**; **3Ln** = **3La**, **3Tb**, **3Ho**, **3Er**, **3Yb**),  $[K\{Ln(tBu_2pz)_4\}]_n$  (**4Ln**; **4Ln** = **4La**, **4Nd**, **4Sm**, **4Tb**, **4Ho**, **4Er**, **4Yb**, **4Lu**), with the last two

classes generally being obtained by loss of toluene from **1Ln** or **2Ln**, and  $[Na(tBu_2pzH)\{Ln(tBu_2pz)_4\}] \cdot PhMe$  (**5Ln**; **5Ln** = **5Nd**, **5Er**, **5Yb**). Extraction with 1,2-dimethoxyethane (DME) after isolation of **2Ho** yielded  $[K(dme)\{Ho(tBu_2pz)_4\}]$  (**6Ho**). X-ray crystal structures of **1Ln** (= **1Tb**, **1Ho**;  $P2_1/c$ ), **2Ln** (= **2La**, **2Sm**, **2Tb**, **2Yb**, **2Lu**;  $Pnma$ ), **3,4Ln** (= **3La**, **3Er**, **4Sm**;  $P2_1/m$ ), and **5Ln** (= **5Nd**, **5Er**, and **5Yb**;  $P\bar{1}$ ) show each group to be isomorphous regardless of the size of the  $Ln^{3+}$  ion. All complexes contain eight-

coordinate  $\{Ln(\eta^2-tBu_2pz)_4\}$  units. These are further linked to the alkali metal by bridging through two (**1,2,5Ln**) or three (**3,4Ln**) *tBu*<sub>2</sub>*pz* groups which show striking coordination versatility. Sodium is coordinated by an  $\eta^4-PhMe$ , a  $\mu-\eta^2:\eta^2-tBu_2pz$ , and a  $\mu-\eta^4(Na):\eta^2(Ln)-tBu_2pz$  ligand in **1Ln**, and by one  $\eta^1-tBu_2pzH$  and two  $\mu-\eta^3(Na):\eta^2(Ln)$  ligands in **5Ln**. By contrast, potassium has one  $\eta^6-PhMe$  and two  $\mu-\eta^5(K):\eta^2(Ln)$  ligands in **2Ln**. Classes **3,4Ln** form polymeric chains with the alkali metal bonded by two  $\mu-\eta^3(NNC-M):\eta^2(Ln)-tBu_2pz$  ligands within  $[MLn(tBu_2pz)_4]$  units which are joined together by  $\eta^1(C)-tBu_2pz-Na$ , K linkages.

**Keywords:** lanthanoids • metathesis • pyrazolates • rare earths • structure elucidation

## Introduction

Use of bulky ligands has enabled the formation of homoleptic divalent and trivalent mononuclear rare-earth organometallic compounds,<sup>[1–4]</sup> organoamides,<sup>[2,4–7]</sup> and organooxometallics,<sup>[2,7–9]</sup>  $[Ln(L)_n]$  ( $L$  = alkyl or aryl,  $NR_2$ , or  $OR$ ;  $n=2$  or 3), for example,  $[Ln\{N(SiMe_3)_2\}_3]$ ,<sup>[10]</sup>  $[Ln(OC_6H_3-2,6-tBu_2-4Me)_3]$ <sup>[11]</sup> and  $[Ln\{C(SiMe_3)_2\}_3]$ ,<sup>[12]</sup> even though the large size

of  $Ln^{3+}$  favors heteroleptic complexes  $[Ln(L)_n(L')_m]$  ( $L'$  = neutral donor, usually a polar solvent).<sup>[1–9]</sup> Coordination/steric saturation requirements may result in association even with bulky ligands, for example,  $[Yb(OAr)_2]$  ( $Ar=C_6H_2-2,6-tBu_2-4-Me$ <sup>[13]</sup> or  $C_6H_3-2,6-Ph_2$ <sup>[14]</sup>), agostic  $Ln \cdots CH$  interactions, for example, in  $[Ln\{CH(SiMe_3)_2\}_3]$ ,<sup>[15]</sup> or intramolecular  $\pi-Ph \cdots Ln$  bonding, for example, in  $[Ln(OC_6H_3-2,6-Ph_2)_2]_3$ .<sup>[14,16]</sup> Homoleptic anionic complexes  $[LnL_3]^-$  or  $[LnL_3]^{2-}$  are attractive targets as they have the advantage of at least one extra ligand to assist coordination/steric saturation and so avoid solvation/ligation by neutral donors.<sup>[2,8]</sup> A number of low-coordinate examples of homoleptic aryloxolanthanoidate(III) complexes are known, for example,  $[MLn(OC_6H_3-2,6-iPr_2)_4]_n$  ( $M=K, Cs$ ),<sup>[17–19]</sup>  $[Cs_2La(OC_6H_3-2,6-iPr_2)_5]_n$ ,<sup>[20]</sup>  $[NaLn(OC_6H_3-2,6-Ph_2)_4]$ ,<sup>[20,21]</sup> and  $[Na(thf)_6][Nd(OC_6H_2-2,6-tBu_2-4-Me)_4]$ .<sup>[22]</sup> In pyrazolatolanthanoid(III) chemistry, (see reference<sup>[23]</sup> and references therein), the only hitherto reported homoleptic anionic lanthanoid complexes

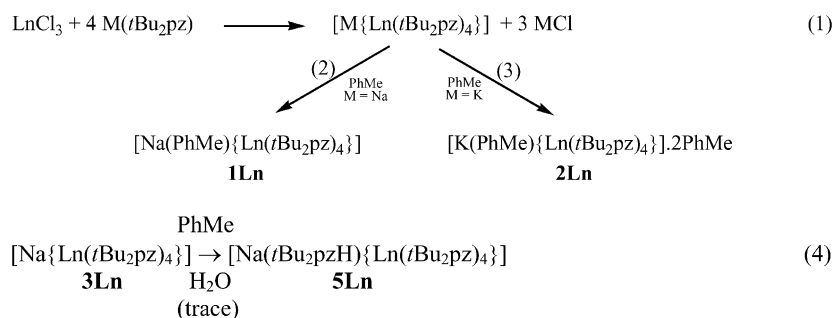
[a] Prof. G. B. Deacon, Dr. E. E. Delbridge, D. J. Evans, Dr. R. Harika, Assoc. Prof. P. C. Junk  
School of Chemistry, Monash University, Victoria 3800 (Australia)  
Fax: (+61) 3-9950-4597  
E-mail: glen.deacon@sci.monash.edu.au  
peter.junk@sci.monash.edu.au

[b] Dr. B. W. Skelton, Prof. A. H. White  
Department of Chemistry, University of Western Australia, Crawley  
WA 6009 (Australia)  
Fax: (+61) 8-9380-1005  
E-mail: ahw@crystal.uwa.edu.au

are  $[\text{K}\{\text{Er}(\text{tBu}_2\text{pz})_4\}]_n^{[24]}$  and  $[\text{K}(\text{[18]crown-6})(\text{dme})(\eta^1\text{-PhMe})][\text{Er}(\text{tBu}_2\text{pz})_4]^{[24]}$  from an exploratory study for the present investigation. The former was obtained by a high temperature, donor-solvent-free metathesis reaction to obviate competition from ether complex formation, for example, giving  $[\text{Ln}(\text{tBu}_2\text{pz})_3(\text{thf})_2]$  or  $[\text{Ln}(\text{tBu}_2\text{pz})_3(\text{dme})]_n^{[25]}$  in the common metathesis donor solvents THF or DME.<sup>[1-4,8]</sup> The supramolecular architecture of  $[\text{K}\{\text{Er}(\text{tBu}_2\text{pz})_4\}]_n^{[24]}$  featured the new  $\mu\text{-}\eta^2\text{:}\eta^3(\text{N}_2\text{C})$  pyrazolate coordination mode and a rare case of  $\eta^1\text{-C}$  ligation,<sup>[23b,26a]</sup> thereby creating interest in the whole  $[\text{M}\{\text{Ln}(\text{tBu}_2\text{pz})_4\}]_n$  (M = alkali metal) structural class. We now report syntheses of a range of these novel heterobimetallic compounds using elevated temperature metathesis, together with the X-ray crystal structures of representative complexes. Sufficient Lewis acidity remains for crystallization from toluene to yield crystallographically characterizable monomeric toluene complexes  $[\text{M}(\text{PhMe})\{\text{Ln}(\text{tBu}_2\text{pz})_4\}]$  which, however, readily revert to  $[\text{M}\{\text{Ln}(\text{tBu}_2\text{pz})_4\}]_n$  species on standing. Overall, the complexes feature several uncommon pyrazolate coordination modes, and develop the emerging richness of pyrazolate ligation, as for example in reference [23,24,26].

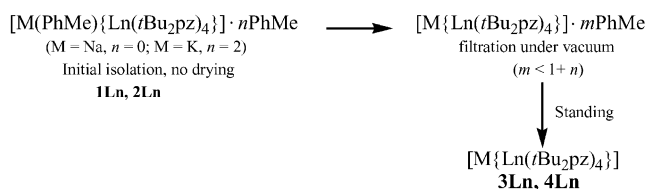
## Results and Discussion

**Syntheses and characterization:** The complexes  $[\text{Na}(\text{PhMe})\{\text{Ln}(\text{tBu}_2\text{pz})_4\}]$  (**1Ln**; **1Ln** = **1Tb**, **1Ho**, **1Er**, **1Yb**) and  $[\text{K}(\text{PhMe})\{\text{Ln}(\text{tBu}_2\text{pz})_4\}] \cdot 2\text{PhMe}$  (**2Ln**; **2Ln** = **2La**, **2Sm**, **2Tb**, **2Ho**, **2Yb**, **2Lu**) were isolated following extraction by toluene of the products of the reaction of anhydrous  $\text{LnCl}_3$  (Ln = La, Nd, Sm, Tb, Ho, Er, Yb, Lu) with four molar equivalents of  $\text{M}(\text{tBu}_2\text{pz})$  (M = Na, K) under vacuum in a sealed Carius tube at elevated temperatures (200–300 °C) [reactions (1)–(3)]. The solvent-free products  $[\text{Na}\{\text{Ln}(\text{tBu}_2\text{pz})_4\}]_n$  (**3Ln**; **3Ln** = **3La**, **3Tb**, **3Ho**, **3Er**, **3Yb**) and  $[\text{K}\{\text{Ln}(\text{tBu}_2\text{pz})_4\}]_n$  (**4Ln**; **4Ln** = **4La**, **4Nd**, **4Sm**, **4Tb**, **4Ho**, **4Er**,<sup>[24]</sup> **4Yb**, **4Lu**) were obtained either straight from the Carius tube (**3Er**), directly from toluene (**3La**, **4Nd**, as reported for **4Er**<sup>[24]</sup>) or by loss of toluene from **1Ln** or **2Ln** upon standing (**3Tb**, **3Ho**, **3Yb**, **4La–Lu** (above) excluding **4Nd**, **4Er**<sup>[24]</sup>). Class **5** complexes  $[\text{Na}(\text{tBu}_2\text{pzH})\{\text{Ln}(\text{tBu}_2\text{pz})_4\}] \cdot \text{PhMe}$  (**5Ln**; **5Ln** = **5Nd**, **5Er**, **5Yb**) crystallized from toluene following attempts to prepare class **1Ln** and **3Ln** complexes. In the case of Ln = Yb, crystallization of **5Yb** was followed by isolation of the target **1Yb** as the bulk product. Class **5Ln** products probably result from adventitious hydrolysis on workup (reaction 4).



Class **4Ln** compounds (source of **2Ln**) were prepared in the presence of 1,2,4,5-tetramethylbenzene (TMB), which was removed by hexane extraction before treatment with toluene. The use of TMB in syntheses of **3Ln** (source of **1Ln**) was abandoned as it offered no major preparative advantages and necessitated removal by an inconvenient sublimation, owing to the slight solubility of **3Ln** in hexane. Low yields (7–21 %) were obtained for products synthesized from commercial (purified)  $\text{LnCl}_3$ , whereas the use of  $\text{LnCl}_3$  generated from  $\text{Ln}_2\text{O}_3$ , HCl and  $\text{NH}_4\text{Cl}$ <sup>[27]</sup> and not purified, gave higher yields of products (60–77 %) under similar conditions, for example, for **4Nd**, (**4Er**<sup>[24]</sup>), and **1Yb**. This could perhaps be a consequence of differences in particle size. The limited solubility of some complexes in toluene may also have contributed to low yields, although the isolated products were generally obtained by two substantial toluene extractions. Following the reaction of  $\text{HoCl}_3$  and  $\text{K}(\text{tBu}_2\text{pz})$ , color remained in the toluene-treated residue, which was then extracted with the more polar solvent DME, giving  $[\text{K}(\text{dme})\{\text{Ho}(\text{tBu}_2\text{pz})_4\}]$  (**6Ho**). A similar extraction from another reaction mixture provided evidence for a heteroleptic pyrazolate chloride and this is to be explored in the future.<sup>[28]</sup> Reaction between  $\text{SmCl}_3$  (as a representative  $\text{LnCl}_3$ ) and  $\text{K}(\text{tBu}_2\text{pz})$  could not be induced in refluxing toluene.

When crystals suitable for X-ray crystallography deposited from toluene, representative specimens (**1Ln**, **2Ln**, **3Ln**) were removed and coated with a perfluoroalkyl ether oil to inhibit loss of toluene (coordinated, or solvent of crystallization). The bulk products from filtration under vacuum generally had a lower toluene content (metal analyses), whilst longer storage resulted in complete desolvation, giving **3Ln** and **4Ln** (<sup>1</sup>H NMR and microanalysis after intercontinental transport) (Scheme 1). Thus, single crystals of



Scheme 1. Progressive loss of toluene from single crystals.

$[\text{K}(\text{PhMe})\{\text{Sm}(\text{tBu}_2\text{pz})_4\}] \cdot 2\text{PhMe}$  (**2Sm**) have been isolated and structurally characterized; the bulk sample initially analysing (% Sm) as  $[\text{K}\{\text{Sm}(\text{tBu}_2\text{pz})_4\}] \cdot 1\frac{1}{2}\text{PhMe}$ , and, on standing, as **4Sm** (<sup>1</sup>H NMR, microanalysis). Crystals of **2Sm** stored under a light perfluoroalkyl ether crumbled to a white powder surrounding a single crystal of **4Sm**, which was structurally characterized, confirming the outcome of toluene loss. Similar behavior was observed for  $[\text{Na}(\text{tBu}_2\text{pzH})\{\text{Nd}(\text{tBu}_2\text{pz})_4\}] \cdot \text{PhMe}$ , **5Nd**,

which underwent partial loss of toluene before microanalysis.

The parent **3Ln**, **4Ln** classes have high thermal stability. Solidification of the reaction mixtures in their syntheses is indicative of melting points/decomposition temperatures above the elevated reaction temperatures (250–300 °C for most complexes; 200 °C for **4Nd**, **4Sm**). The representative toluene complex **2La** lost toluene at 60 °C without melting (giving **4La**) and remained unmelted at 300 °C. The visible/near-infrared absorption spectra of complexes containing  $\text{Ho}^{3+}$ ,  $\text{Er}^{3+}$ ,  $\text{Nd}^{3+}$ ,  $\text{Sm}^{3+}$ ,  $\text{Yb}^{3+}$  showed absorptions characteristic of the appropriate  $\text{Ln}^{3+}$  ion.<sup>[29]</sup> As the formation of toluene complexes (reactions (2) and (3)) shows, dissolution of **3Ln**, **4Ln** in  $\text{C}_6\text{D}_6$  for NMR measurements must disrupt the solid-state structures giving  $\text{C}_6\text{D}_6$  complexed species.  $^1\text{H}$  NMR spectra of **3La**, **4La**, **4Nd**, **4Sm**, and **4Lu** showed no toluene peaks, with two resonances integrating 18:1, attributable to the *t*Bu protons and the pyrazolate H4 protons respectively. In the case of **4La**, **4Sm**, and **4Lu**, this provided evidence for ease of loss of toluene from the corresponding **2Ln** derivatives. A large paramagnetic shift was observed for H4 of **4Nd**, though less than for  $[\text{Nd}_2(\text{tBu}_2\text{pz})_6]^{[30]}$  whilst H4 of **4Sm** differed little from diamagnetic values as previously noted for  $[\text{Sm}(\text{Ph}_2\text{pz})_3]^{[31]}$ . Solubility limitations prevented  $^{13}\text{C}$  NMR measurements in solvents where solid-state structural integrity might be maintained. Infrared spectra were typical of *t*Bu<sub>2</sub>pz complexes, as for instance in reference [24,30,32]. Some complexes showed very weak to weak absorption around  $3230\text{ cm}^{-1}$ , indicative of  $\nu(\text{N}-\text{H})$  due to trace *t*Bu<sub>2</sub>pzH. It was probably formed by slight hydrolysis during the recording of the spectrum of the Nujol mull, which usually provides adequate protection for a short scan time. For **5Nd** and **5Er**, which contain coordinated pyrazole, this band was more intense.

**Crystal structure investigations: Overview:** X-ray structure determinations have been carried out for the complexes, **1Tb**, **1Ho**, **2La**, **2Sm**, **2Tb**, **2Yb**, **2Lu**, **3La**, **3Er**, **4Sm**, **5Nd**, **5Er**, and **5Yb**. All systems feature an  $\text{M}\cdots\text{Ln}$  axis ( $\text{M}=\text{Na}/\text{K}$ ) surrounded by an array of ligands, heavily substituted by *tert*-butyl groups, so that the peripheral aspect is that of a hydrocarbon cylinder (Figures 1–4). *tert*-Butyl groups are notoriously prone to (temperature-dependent<sup>[32]</sup>) rotational disorder in the lattice. In the recent determination of  $[\text{Eu}_4(\text{tBu}_2\text{pz})_8]^{[32]}$  the model adopted was that of an array of ligands about a core line of metal atoms, rotationally disordered over pairs of sites rotated by approximately 90° within an essentially common peripheral sheath of methyl groups. Two of the present structural types have been modeled in this way—the orthorhombic *Pnma* series, found for **2Ln**, and the monoclinic *P2<sub>1</sub>/m* array of **3Ln** or **4Ln**. In both cases, the metal-atom dispositions (within a crystallographic mirror plane in each case) are such as to frustrate attempts to define better models in space groups of lower symmetry, even if such models were correct. Disordered models have ultimately, if somewhat unwillingly, been adopted. (In particular, the *P2<sub>1</sub>/m* array is uneasily juxtaposed alongside the previous *P2<sub>1</sub>/c* determination for **4Er**<sup>[24]</sup> ( $a=20.7775(10)$ ,  $b=12.3035(6)$ ,  $c=18.8274(6)$  Å,  $\beta=$

$90.527(1)^\circ$ ,  $V=4813\text{ \AA}^3$ ;  $T$  approximately 123 K)). In each case, the structure is described in terms of one of the pair of deconvoluted, equivalent components.

Pertinent bond lengths and angles are given in Table 1 and Table 2 for **1Tb** and **1Ho**, in Table 3 and Table 4 for **2La** and **2Lu**, in Table 5 and Table 6 for **3La**, **3Er** and **4Sm**, and in Table 7 and Table 8 for **5Nd** and **5Yb**.

All complexes contain  $\text{MLn}(\text{tBu}_2\text{pz})_4$  ( $\text{M}=\text{Na}, \text{K}$ ) units. In **1Ln**, **2Ln**, and **5Ln**, they form discrete heterobimetallic monomers  $[\text{M}(\text{L})\{\text{Ln}(\text{tBu}_2\text{pz})_4\}]$  (**1Ln**:  $\text{M}=\text{Na}$ ,  $\text{L}=\text{PhMe}$ , (Figure 1); **2Ln**:  $\text{M}=\text{K}$ ,  $\text{L}=\text{PhMe}$ , (Figure 2); **5Ln**:  $\text{M}=\text{Na}$ ,  $\text{L}=\eta^1(\text{N})\text{-tBu}_2\text{pzH}$ , (Figure 4)), whilst in **3Ln** ( $\text{M}=\text{Na}$ ) and **4Ln** ( $\text{M}=\text{K}$ ), the  $\text{MLn}(\text{tBu}_2\text{pz})_4$  units are linked into one-dimensional chains by  $\pi\text{-}\eta^1\text{-}(\text{tBu}_2\text{pz})(\text{C})\text{-M}$  interactions (Figure 3). These linkages replace the ligands L of **1Ln**, **2Ln**, and **5Ln**. Within each series **1Ln**, **2Ln**, **3Ln**, **4Ln**, and **5Ln**, the complexes are isomorphous despite the variation in  $\text{Ln}^{3+}$  size.

**Lanthanoid coordination:** In all cases, the lanthanoid metal centre is surrounded by four nitrogen-bound  $\eta^2\text{-tBu}_2\text{pz}$  ligands forming eight coordinate  $[\text{Ln}(\text{tBu}_2\text{pz})_4]^-$  moieties, with two of the pyrazolate ligands bridging to the alkali metal to form the  $[\text{MLn}(\text{tBu}_2\text{pz})_4]$  units. Chelation of the ligand to the lanthanoid is symmetrical, especially for **1Ln** and **2Ln**, the maximum difference in the two Ln–N distances being approximately 0.1 Å for the bridging ligands of **5Ln** and 0.055–0.090 Å for one bridging ligand of **3Ln**. In general, average Ln–N bond lengths for the bridging ligands are longer (0.05–0.10 Å, but 0.12–0.14 Å for one bond of **3Ln**) than those of terminal pyrazolates, as expected. However, **2Ln** complexes have only small differences and have the most regular  $\text{LnN}_8$  coordination. Corresponding Ln–N bonds within each structural series show the appropriate size variation for the change in  $\text{Ln}^{3+}$  ionic radius.<sup>[33]</sup> With allowances for the differences in ionic radii, the average Ln–N bond lengths are similar to those found in the discrete  $[\text{Er}(\text{tBu}_2\text{pz})_4]^-$  ions in the charge separated  $[\text{K}([\text{18}]\text{crown-6})(\text{dme})(\eta^1\text{-MePh})][\text{Er}(\text{tBu}_2\text{pz})_4]^{[24]}$  and of the eight coordinate  $[\text{Er}(\eta^2\text{-tBu}_2\text{pz})_3(\text{thf})_2]^{[25a]}$  although the crowding in the heteroleptic complex is significantly greater than in  $[\text{Ln}(\eta^2\text{-tBu}_2\text{pz})_4]^-$ .<sup>[34]</sup> (On the basis of cone-angle-factor calculations,<sup>[34a]</sup> the steric coordination number of *t*Bupz is approximately 1.8 compared with 1.21 for THF.<sup>[34b]</sup>) Despite the difference in the alkali metal, the average Tb–N bond lengths of **1Tb** and **2Tb** are similar (Tables 1 and 3). The arrangement of the eight nitrogen atoms around the lanthanoid is intermediate between a dodecahedral and square antiprismatic arrangement,<sup>[35]</sup> with **1Ln** and **5Ln** closer to the former and **2Ln** and **3Ln** to the latter. The arrangements of the midpoints of the N–N bonds of the pyrazolate ligands about  $\text{Ln}^{3+}$  are irregular. There are four centroid–Ln–centroid angles that range from 85.8–107.9°, and two that range from 135.7–142.4°, reflecting major deviations from either tetrahedral or square planar geometry.

These homoleptic  $\eta^2$  attachments of four pyrazolate ligands around  $\text{Ln}^{3+}$  are unique in lanthanoid pyrazolate chemistry, apart from **4Er** and  $[\text{K}([\text{18}]\text{crown-6})(\text{dme})(\eta^1\text{-MePh})][\text{Er}(\text{tBu}_2\text{pz})_4]$  of our preliminary communication.<sup>[24]</sup> The arrangement is similar to that found in the first homo-

leptic  $\eta^2$ -pyrazolato complexes, as for instance  $[\text{Ti}(\eta\text{-R}_2\text{pz})_4]$  ( $\text{R}_2\text{pz}$  = 3,5-dimethyl- or 3,5-diphenylpyrazolate)<sup>[36]</sup> and in the analogous  $[\text{Zr}(\text{Hf})(t\text{Bu}_2\text{pz})_4]$  derivatives.<sup>[37]</sup> Amongst homoleptic neutral rare-earth pyrazolates  $[\text{Ln}(\text{R}_2\text{pz})_3]$ , only  $[\text{Sc}(\eta^2\text{-}t\text{Bu}_2\text{pz})_3]$  has solely  $\eta^2$ -bonded ligands,<sup>[32]</sup> attributable to the relatively small size of  $\text{Sc}^{3+}$ . Other homoleptic complexes are at least dimeric, with  $\mu\text{-R}_2\text{pz}$  groups linking Ln metals and more than one type of pyrazolate bonding to Ln.<sup>[23d,30,32]</sup> In contrast, heteroleptic complexes  $[\text{Ln}(\text{R}_2\text{pz})_3(\text{L})_m]$ , for example  $\text{L} = \text{THF}$ , DME, generally have  $\eta^2$ -pyrazolates.<sup>[23a,c,25,38,39]</sup> Unlike the consistent lanthanoid coordination spheres in **1–5Ln**, the environments around the alkali metal vary and are described with the individual compound classes.

$[\text{Na}(\text{PhMe})\{\text{Ln}(t\text{Bu}_2\text{pz})_4\}]$  (**1Ln** = **1Tb**; **1Ho**): In these isomorphous (monoclinic, space group  $P2_1/c$ ) discrete monomeric heterobimetallic complexes, anionic  $[\text{Ln}(t\text{Bu}_2\text{pz})_4]^-$  units are linked through a pair of bridging pyrazolate ligands to  $\text{Na}(\text{PhMe})^+$  groups (Figure 1; Tables 1 and 2). Coordination of toluene to sodium is evident by its location covering an otherwise naked face of  $\text{Na}^+$ , and by the near-perpendicular intersection angle between the Na–arene ring centroid vector and the toluene-ring plane ( $78.7$ ,  $79.1^\circ$ ). With four Na–C(Ph) contacts in the range  $2.779(3)$ – $3.015(2)$  Å for C(102–105) (Table 2), and two others approximately  $0.2$  Å larger ( $3.178(3)$ – $3.242(2)$  Å, C(101, 106)), either  $\eta^4$  or  $\eta^6$  coordination can be considered. There are four relevant reported structures, namely, four-coordinate  $\text{Na}^+$  in  $[\text{Na}(\eta^6\text{-PhMe})\text{Sn}(\text{Si}(\text{SiMe}_3)_3)_3]$  (**A**),<sup>[40]</sup> five-coordinate  $\text{Na}^+$  in  $[\text{Na}(\eta^4\text{-PhMe})\text{GaMe}_3(\text{Si}(\text{SiMe}_3)_3)]$  (**B**),<sup>[41]</sup> six-coordinate  $\text{Na}^+$  in  $[\text{Na}_6(\eta^6\text{-PhMe})_2(\text{SSiPh}_3)_6]$  (**C**),<sup>[42]</sup> and eight-coordinate  $\text{Na}^+$  in  $[\text{Na}(\eta^6\text{-PhMe})_2\text{Al}(\text{SiMe}_3)_4]$  (**D**).<sup>[43]</sup> These have bonding Na–C interactions of  $2.82(5)$ – $2.94(4)$  Å in **A**,<sup>[40]</sup>  $2.85$ – $3.02$  Å in **B**<sup>[41]</sup> ( $\eta^4$ , with contacts at  $3.13$ ,  $3.23$  Å considered nonbonding),<sup>[41]</sup>  $2.896(4)$ – $3.115(3)$  Å in **C** (also with  $2.852(2)$ – $3.664(3)$  Å intramolecular  $\pi\text{-Ph-Na}$  contacts of  $\text{SSiPh}_3$  regarded as interactions),<sup>[42]</sup> and  $2.80(4)$ – $3.27(4)$  Å in

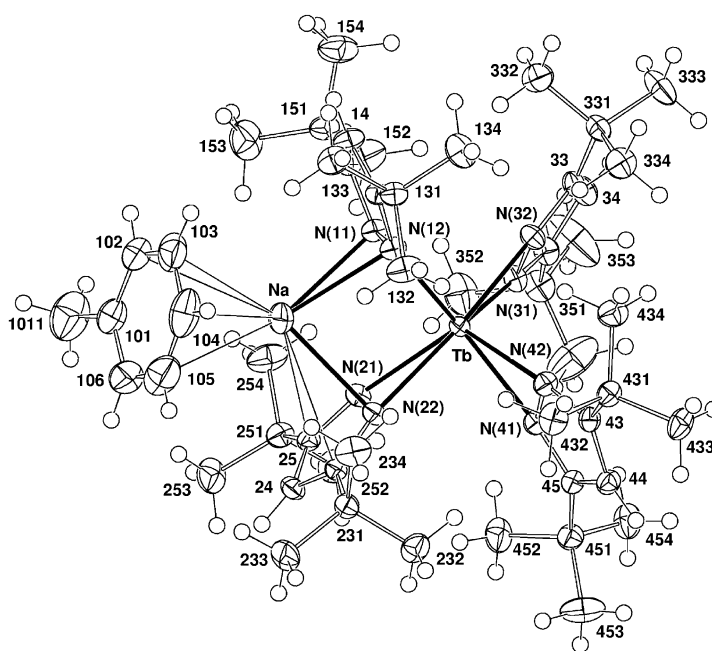


Figure 1. X-ray crystal structure of  $[\text{Na}(\eta^4\text{-PhMe})\{\text{Tb}(t\text{Bu}_2\text{pz})_4\}]$  (**1Tb**), representative of **1Ln**.

Table 1. The lanthanoid environments in  $[\text{Na}(\text{PhMe})\{\text{Ln}(t\text{Bu}_2\text{pz})_4\}]$  (**1Ln**; **1Ln** = **1Tb**, **1Ho**).  $r$  is the lanthanoid metal–ligand distance [Å]; other entries in the matrix are the angles subtended by the relevant atoms at the head of the rows and columns. Values are listed in the order, **1Tb**, **1Ho**. Tables 3, 5, and 7 are presented similarly.<sup>[a]</sup>

Atom	$r$	N(12)	N(21)	N(22)	N(31)	N(32)	N(41)	N(42)
N(11)	2.451(1)	33.13(5)	84.04(4)	92.88(4)	93.95(5)	82.95(5)	171.65(5)	139.97(5)
	2.425(2)	33.47(7)	84.01(7)	93.11(7)	94.17(7)	83.18(7)	172.00(8)	139.69(7)
N(12)	2.445(1)		95.21(4)	85.33(4)	119.07(4)	94.24(5)	139.23(5)	107.78(5)
	2.416(2)		95.75(7)	85.67(7)	119.51(7)	94.46(7)	139.19(7)	107.20(7)
N(21)	2.444(1)			33.33(5)	109.43(5)	139.80(5)	94.87(5)	117.25(5)
	2.417(2)			33.83(7)	108.59(8)	139.20(7)	95.16(7)	118.03(7)
N(22)	2.405(1)				140.76(5)	172.76(5)	81.86(5)	90.41(5)
	2.377(2)				140.27(8)	172.81(7)	81.98(7)	90.69(7)
N(31)	2.356(1)					34.47(5)	94.22(5)	108.15(5)
	2.340(2)					34.63(8)	93.63(7)	107.97(7)
N(32)	2.339(1)						102.93(5)	96.59(5)
	2.313(2)						102.37(7)	96.13(8)
N(41)	2.341(1)							34.36(5)
	2.309(2)							34.81(7)
N(42)	2.361(1)							
	2.340(2)							

[a] Na...Tb, Ho are  $3.4746(8)$ ,  $3.462(1)$  Å.

**D**.<sup>[43]</sup> Given that the  $\text{Na}^+$  ion in the present complexes is at least 'six-coordinate' (see below), the four shorter C(PhMe)–Na contacts of **1Ln** are certainly bonding, giving  $\eta^4\text{-PhMe}$ , although  $\eta^6\text{-PhMe}$  is plausible.

Although the bridging  $t\text{Bu}_2\text{pz}$  ligands (1 and 2) have similar Ln–N distances, they differ in their binding modes to  $\text{Na}^+$  (Figure 1). The former approaches normal to the Na–Ln vector, consistent with  $\mu\text{-}\eta^2(\text{N}_2)\text{:}\eta^2(\text{N}_2)$  binding, but with a tilt towards the  $\text{Na}^+$  ion (ligand plane–Na–Ln vector intersection angle  $64.6(\times 2)^\circ$ ). However, ligand 2 lies below the  $\text{Na}^+$  ion such that the Na–center(N–N bond)–centroid( $t\text{Bu}_2\text{pz}$ ) angle is  $94.7$ , with  $94.2^\circ$  suggestive of Na– $t\text{Bu}_2\text{pz}$   $\pi$ -bonding. (It is near coplanar with Ln (angle between ligand and LnN<sub>2</sub> planes  $\approx 9^\circ$ ) indicative of Ln–N  $\sigma$  bonding.) From the criteria above for Na–C(PhMe) ligation, Na has

Table 2. Selected sodium–carbon and sodium–nitrogen distances [Å] in [Na(PhMe){Ln(*t*Bu<sub>2</sub>pz)<sub>4</sub>}] (**1Ln**; **1Ln** = **1Tb**; **1Ho**).<sup>[a]</sup>

Na–A, A =	<b>1Tb</b>	<b>1Ho</b>
N(11)	2.494(2)	2.488(3)
N(12)	2.638(2)	2.639(3)
N(21)	2.500(2)	2.501(2)
N(22)	2.545(1)	2.541(2)
C(15) <sup>[b]</sup>	3.232(2)	3.227(3)
C(23)	3.082(2)	3.061(3)
C(24) <sup>[b]</sup>	3.350(2)	3.329(3)
C(25)	3.014(2)	3.007(3)
C(101)	3.242(2)	3.232(4)
C(102)	3.015(2)	3.007(4)
C(103)	2.798(3)	2.797(4)
C(104)	2.779(3)	2.791(4)
C(105)	2.957(3)	2.974(5)
C(106)	3.178(3)	3.184(5)

[a] Angles at Na: C(0)–Na–C(10) 118.1, 118.4; C(0)–Na–C(20) 118.3, 118.6; C(10)–Na–C(20) 122.4, 121.9;  $\Sigma$ 358.8, 358.9. [b] “Nonbonding”.

bonding contacts to C(23) and C(25) (Table 2), in addition to ligation of the pyrazolate nitrogen atoms, so that the coordination mode is  $\mu$ - $\eta^2$ : $\eta^4$ . Ligand 2 has near symmetrical Na–N binding, but for ligand 1 the bond lengths differ by 0.13 Å. As a consequence of this asymmetry, C(15) approaches the Na<sup>+</sup> ion, but not sufficiently so as to be viewed as a significant interaction (Table 2). With  $\pi$ - $\eta^4$ (CNNC)⋯Na binding of ligand 2,  $\eta^2$ (N<sub>2</sub>) coordination of ligand 1, and  $\eta^4$  ligation of toluene, the sodium is six-coordinate (or seven, if PhMe is considered  $\eta^6$  linked). The centroids of PhMe and *t*Bu<sub>2</sub>pz ligands 1 and 2 have a near-trigonal planar distribution around sodium (118.1–122.4°;  $\Sigma$ 358.8, 358.9°) in **1Ln** complexes.

[K(PhMe){Ln(*t*Bu<sub>2</sub>pz)<sub>4</sub>}]·2PhMe (**2Ln**; **2Ln** = **2La**, **2Sm**, **2Tb**, **2Yb**, **2Lu**): The isomorphous series (orthorhombic, space group *Pnma*) of discrete monomeric bimetallic complexes (Figure 2; Tables 3 and 4), embraces the full gamut of Ln<sup>3+</sup> sizes. Both the Ln<sup>3+</sup> ion and the K<sup>+</sup> ion reside on a crystallographic mirror plane, with half of the molecular formula comprising the asymmetric unit. There are three unique pyrazolate ligands (two (1,2) bridging Ln<sup>3+</sup> and K<sup>+</sup>) with the fourth generated by reflection of the terminal ligand 3, (N(31,32), C(33–35)).

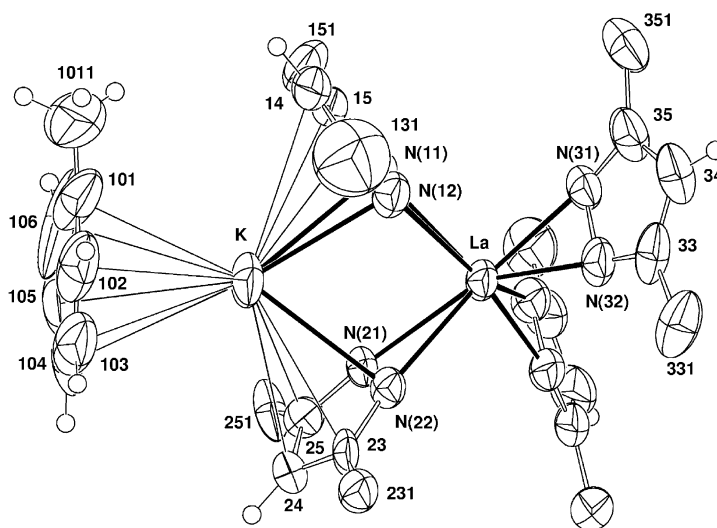


Figure 2. X-ray crystal structure of [K( $\eta^6$ -PhMe)[La(*t*Bu<sub>2</sub>pz)<sub>4</sub>]] (**2La**) representative of **2Ln**. Methyl groups are omitted from the *t*Bu groups for clarity

Table 3. The lanthanoid environment in [K(PhMe){Ln(*t*Bu<sub>2</sub>pz)<sub>4</sub>}]·2PhMe (**2Ln** = **2La** (first entries), **2Lu**). Arranged as in Table 1. (Data for **2Sm**, **2Tb**, **2Yb** are available from the deposition).<sup>[a]</sup>

Atom	<i>r</i>	N(12)	N(21)	N(22)	N(31)	N(32)
N(11)	2.520(9)	31.5(3)	83.0(3)	93.8(3)	90.0(2)	114.3(2)
	2.35(1)	33.4(4)	86.1(4)	98.5(4)	88.6(3)	115.0(3)
N(12)	2.55(1)		87.6(3)	81.3(3)	80.6(2)	92.6(3)
	2.33(1)		90.6(4)	83.9(4)	80.3(4)	92.31(3)
N(21)	2.527(9)			32.2(3)	166.7(2)	144.0(2)
	2.35(1)			34.0(4)	170.0(4)	142.8(3)
N(22)	2.519(8)				138.2(2)	112.4(2)
	2.37(1)				139.3(3)	109.7(3)
N(31)	2.499(5)					32.1(1)
	2.327(8)					34.7(2)
N(32)	2.487(5)					
	2.318(6)					

[a] K⋯La, Lu are 4.067(2), 3.947(3) Å.

Coordination of toluene to the K<sup>+</sup> ion is indicated by its position on an otherwise naked face, by intersection of the toluene ligand planes by the K–centroid(PhMe) vectors at near 90° (87.2–88.8°), and by six similar K–C(Ph) contacts (Table 4) for each compound (range 3.21(1)–3.39(1) Å) indicative<sup>[44–51]</sup> of bonding. Comparable K–C bond lengths have been reported in, for example, seven-coordinate [K( $\eta^6$ -PhMe)( $\mu$ -Cl){Lu(CH(SiMe<sub>3</sub>)<sub>2</sub>)<sub>3</sub>}] (six K–C bonds at 3.161–3.513 Å),<sup>[44]</sup> six-coordinate [K( $\eta^6$ -PhMe){Si<sub>2</sub>(SiMe<sub>3</sub>)<sub>3</sub>}] (six K–C bonds: 3.20–3.41(esds not given) Å),<sup>[49]</sup> and nine-coordinate [K( $\eta^6$ -PhMe){[18]crown-6}]<sup>+</sup> (six at 3.044(5)–3.311(5) Å).<sup>[47]</sup> These data are indicative of  $\eta^6$  coordination of toluene in **2Ln**. Further, the difference between the K–C distances of **2Ln** and the ( $\eta^4$ ) Na–C bonds of **1Ln** are consistent with appropriate ionic radii differences.<sup>[33]</sup>

Although ligands 1 and 2 are crystallographically different, they bind in a similar way to K<sup>+</sup>. Each is coordinated through two nitrogen atoms with slight asymmetry (0.12–0.17 Å) and through three carbon atoms, so that the ligands exhibit  $\mu$ - $\eta^2$ : $\eta^5$  coordination, a binding mode recently observed in [Eu<sub>4</sub>(*t*Bu<sub>2</sub>pz)<sub>8</sub>]<sup>[32]</sup> and [Ba<sub>6</sub>(thf)<sub>6</sub>(Me<sub>2</sub>pz)<sub>8</sub>]{(OSiMe<sub>2</sub>)<sub>2</sub>O<sub>2</sub>}]<sup>[26f]</sup> (Me<sub>2</sub>pz = 3,5-dimethylpyrazolate). Both ligands are near coplanar with Ln (Ln deviations: 0.18(2)–0.29(2) Å), and near perpendicular to K<sup>+</sup>, the K–(ring-plane

Table 4. Selected potassium–carbon and potassium–nitrogen distances [Å] in [K(PhMe){Ln(*t*Bu<sub>2</sub>pz)<sub>4</sub>}] (**2Ln**; **2Ln**=**2La**, **2Lu**). (Data for **2Sm**, **2Tb**, **2Yb** are available from the deposition).<sup>[a]</sup>

K–A, A =	<b>2La</b>	<b>2Lu</b>
N(11)	2.984(9)	2.99(1)
N(12)	2.83(1)	2.83(1)
N(21)	2.858(9)	2.84(1)
N(22)	2.978(8)	3.01(1)
C(13)	3.09(1)	3.07(1)
C(14)	3.41(1)	3.33(2)
C(15)	3.34(1)	3.24(2)
C(23)	3.32(1)	3.30(2)
C(24)	3.41(1)	3.39(1)
C(25)	3.15(1)	3.22(2)
C(101)	3.21(1)	3.28(1)
C(102)	3.22(1)	3.30(1)
C(103)	3.36(1)	3.33(1)
C(104)	3.33(1)	3.32(2)
C(105)	3.30(2)	3.28(1)
C(106)	3.31(2)	3.27(1)

[a] Angles at K: C(0)–K–C(10) 127.5, 128.0; C(0)–K–C(20) 122.5, 125.4; C(10)–K–C(20) 109.3, 105.2;  $\Sigma$  359.3, 358.6.

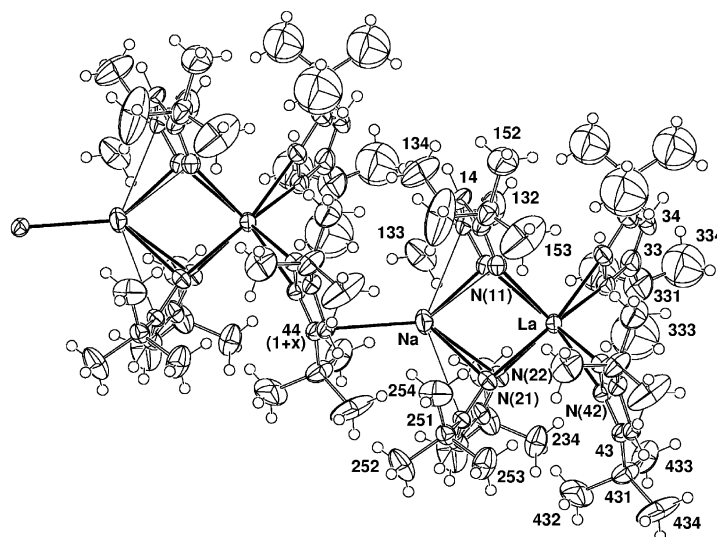


Figure 3. X-ray crystal structure of [Na{La(*t*Bu<sub>2</sub>pz)<sub>4</sub>}]<sub>n</sub> (**3La**), representative of **3Ln**, **4Ln**.

centroid) vector/ligand plane intersection angles approaching approximately 90°. Thus,  $\pi$ - $\eta^5$  bonding is indicated. The K–C(*t*Bu<sub>2</sub>pz) distances (Table 4) are comparable with K–C(PhMe) bond lengths, with the former showing greater variation. Thus, for example, the shortest K–C(*t*Bu<sub>2</sub>pz) distance is 0.12–0.22 Å shorter than the shortest K–C(PhMe) bond length, and the longest is 0.05–0.08 Å longer than the longest K–C(PhMe) distance. However, the average K–C(*t*Bu<sub>2</sub>pz) bond length of the pyrazolate ligands, separately or together, is smaller or the same as the average K–C(PhMe) bond lengths for each of the five **2Ln** compounds. With ligands 1 and 2 thus displaying  $\eta^5$ -K coordination, the potassium ion has a formal nine-coordination arrangement in each **2Ln** complex. There is a near-triangular planar arrangement of the centroids of PhMe and the *t*Bu<sub>2</sub>pz ligands 1 and 2 about potassium (105.2–128.0°), with the sum > 358°.

[Na{Ln(*t*Bu<sub>2</sub>pz)<sub>4</sub>}]<sub>n</sub> (**3Ln**; **3Ln**=**3La**, **3Er**) and [K{Ln(*t*Bu<sub>2</sub>pz)<sub>4</sub>}]<sub>n</sub> (**4Ln**; **4Ln**=**4Sm**): Despite the variation of alkali metal, these complexes are isomorphous (monoclinic *P*<sub>2</sub>/*m*), with one half of the molecular formula comprising the asymmetric unit. In contrast to **1Ln**, **2Ln**, and **5Ln**, three ligands (1, 2, 4) are bridging. A mirror plane lies normal to and bisects ligands 3 and 4, which are thus symmetrically chelated to Ln. C(44) is situated in the mirror plane, binding to an adjacent M<sup>+</sup> and linking the [M{Ln(*t*Bu<sub>2</sub>pz)<sub>4</sub>}] molecules (Figure 3; Tables 5 and 6). Al-

Table 5. The lanthanoid environment in [Na{Ln(*t*Bu<sub>2</sub>pz)<sub>4</sub>}]<sub>n</sub> (**3Ln**; **3Ln**=**3La**, **3Er**) and [K{Sm(*t*Bu<sub>2</sub>pz)<sub>4</sub>}]<sub>n</sub> (**4Sm**). Values are listed in the order **3La**, **3Er**, **4Sm**.<sup>[a]</sup>

Atom	<i>r</i>	N(12)	N(21)	N(22)	N(32)	N(32) <sup>[b]</sup>	N(42)	N(42) <sup>[b]</sup>
N(11)	2.639(4)	31.0(1)	85.3(1)	102.6(1)	113.2(1)	87.38(9)	135.1(1)	106.4(1)
	2.483(6)	33.3(2)	86.8(2)	106.1(2)	115.5(2)	87.0(2)	135.2(2)	103.9(2)
	2.49(2)	33.0(6)	86.3(5)	102.6(5)	117.2(5)	90.9(4)	135.2(5)	105.7(4)
N(12)	2.584(4)		81.3(1)	83.7(1)	97.4(1)	84.98(9)	160.61(9)	137.1(1)
	2.392(7)		83.6(2)	85.5(2)	98.2(2)	84.9(2)	163.5(2)	137.1(2)
	2.48(2)		88.2(5)	87.1(5)	96.0(4)	83.3(4)	165.9(4)	138.5(4)
N(21)	2.521(3)			32.1(1)	141.4(1)	163.8(1)	84.0(1)	93.9(1)
	2.352(5)			34.8(2)	141.5(2)	166.9(2)	83.7(2)	94.4(2)
	2.46(1)			32.7(5)	140.9(4)	168.2(4)	82.4(4)	93.9(4)
N(22)	2.507(4)				109.3(1)	137.6(1)	90.6(1)	114.0(1)
	2.362(6)				106.7(2)	137.8(2)	90.1(2)	116.2(2)
	2.47(2)				108.5(4)	138.1(4)	90.5(5)	115.6(5)
N(32)	2.473(2)					32.76(7)	101.94(6)	111.19(6)
	2.308(3)					35.1(2)	98.3(2)	108.8(1)
	2.395(7)					33.0(6)	97.9(3)	107.5(2)
N(42)	2.522(2)							31.78(6)
	2.354(3)							34.1(1)
	2.449(9)							33.0(2)

[a] Na...La, Er; K...Sm are 3.733(1), 3.656(2); 4.039(3) Å. [b] Symmetry operation: *x*, 1/2–*y*, *z*.

Table 6. Selected alkali metal–carbon and alkali metal–nitrogen distances [Å] in [Na{Ln(*t*Bu<sub>2</sub>pz)<sub>4</sub>}]<sub>n</sub> (**3Ln**; **3Ln**=**3La**, **3Er**) and [K{Ln(*t*Bu<sub>2</sub>pz)<sub>4</sub>}]<sub>n</sub> (**4Ln**; **4Ln**=**4Sm**, **4Er**).

M–A, A =	<b>3La</b>	<b>3Er</b>	<b>4Sm</b>	<b>4Er</b> <sup>[24]</sup>
N(11)	3.025(4)	3.023(6)	3.19(2)	3.077(7)
N(12)	2.399(4)	2.423(6)	2.82(1)	2.812(7)
N(21)	2.510(4)	2.514(7)	2.86(2)	2.842(6)
N(22)	2.828(4)	2.843(6)	3.12(2)	3.130(6)
C(43) <sup>[a]</sup>	3.429(2)	3.551(4)	3.615(9)	3.577(7)
C(44)	2.829(3)	2.926(6)	3.18(1)	3.162(7)
C(45) <sup>[a]</sup>	> 4.1	> 4.1	> 4.1	3.665(7)
C(13)	3.008(5)	2.928(7)	3.16(2)	3.187(7)
C(14) <sup>[a]</sup>	3.810(6)	3.670(8)	3.65(2)	3.549
C(15) <sup>[a]</sup>	3.787(5)	3.698(8)	3.67(2)	3.522
C(23) <sup>[a]</sup>	3.492(4)	3.378(8)	3.55(2)	3.582
C(24) <sup>[a]</sup>	3.610(5)	3.419(9)	3.60(2)	3.496
C(25)	3.060(6)	2.938(9)	3.22(2)	3.093(8)

[a] "Nonbonding".

though **3Ln** and **4Sm** are not isomorphous with **4Er**,<sup>[24]</sup> (see overview) the structures are similar.

The alkali metal is sandwiched between a pair of NNC-bound bridging ligands (1,2) with one M–N bond length (Table 6) much shorter (ligand 1: 0.36–0.62 Å; 2: 0.24–0.33 Å) than the other. Furthermore, the shorter bond is similar to or shorter (by up to 0.15 Å) than the corresponding M–N distance of **1Ln** or **2Ln**. The M–C(13,25) separations (Table 6) for the carbon atoms adjoining the more closely bound nitrogen atoms (12, 21 of ligands 1 and 2) are similar, both to the longer M–N bond lengths (to N(11,22)) and to the corresponding M–C(PhMe) distances of **1Ln** or **2Ln**. Thus, they should be regarded as bonding, leading to  $\eta^3$ (*t*Bu<sub>2</sub>pz) binding to Na or K, and overall  $\mu$ - $\eta^2$ : $\eta^3$ -pyrazolate ligation. All other M–C separations (to C(14,15,23,24)) are at least >0.3 Å longer than M–C(13,25). With M–N(12 or 21)-centroid(*t*Bu<sub>2</sub>pz) angles of 112.5, 97.3 (**3La**), 106.0, 91.9 (**3Er**) and 92.5, 88.7° (**4Sm**), the  $\eta^3$ (*t*Bu<sub>2</sub>pz)–M interaction can be regarded as  $\pi$  bonding. Although Na–N bond differences of up to 0.6 Å (above) strain the concept of the longer distance as bonding, it gains support from there being a bonding carbon atom (C(13,25)) at a comparable distance as part of the  $\pi$ -NNC interaction. In addition, unsymmetrical  $\eta^2$ -R<sub>2</sub>pz or  $\eta^2$ -triazolate coordination with M–N bond-length differences of 0.45 Å for Al–N,<sup>[52]</sup> and approximately 0.60 Å for K–N bonding,<sup>[53]</sup> (but not 0.70 Å for Mg–N in [Mg(*t*Bu<sub>2</sub>pz)<sub>2</sub>(*t*Bu<sub>2</sub>pzH)<sub>2</sub>]<sup>[54]</sup>) has been reported. The large asymmetry (approximately 0.6 Å) in the Na–N<sub>2</sub> binding for ligand 1 in **3La**, **Er** is accompanied by a close Na...*t*Bu contact (to Me(133) of the *tert*-butyl nearest to the shorter Na–N distance; 2.399(4) (**3La**), 2.423(6) Å (**3Er**)). While the exact value of Na–C(133) (**3La**: 2.915(8); **3Er**: 2.87(1) Å) may be influenced by high local displacement parameters, the plausibly agostic (see for example reference [18] for analogous *i*Pr–Ln interactions) contact seems the probable cause of distortion. For ligand 2 of **3La**, **Er** and both ligands 1 and 2 of **4Sm** and **4Er**,<sup>[24]</sup> where the NaN<sub>2</sub> binding asymmetry is less (< 0.35 Å, Table 6), such close Ln–Me contact does not exist.

For the “supramolecular” C–M interaction, the C(44)–Na bond lengths of **3La** and **3Er** are near the shorter  $\eta^4$ -PhMe–

Na distances of **1Ln**. The C(44)–K bond length of **4Sm** (and **4Er**)<sup>[24]</sup> is shorter than all  $\eta^6$ -PhMe–K bond lengths of **2Ln**, providing unequivocal evidence of  $\eta^1$ -C(*t*Bu<sub>2</sub>pz)–M ligation. The M–C(44)-centroid(*t*Bu<sub>2</sub>pz) angles (111.4 (**3La**), 114.9 (**3Er**); 101.9° (**4Sm**)) are consistent with  $\pi$  interactions. The C(43,45)–M distances are  $\geq 0.4$  Å longer and hence are nonbonding. Large C(44)–M–N(12,21) angles (141.5, 132.2 (**3La**), 142.9, 136.8 (**3Er**); 153.4, 130.1° (**4Sm**)) reflect repulsion between the *t*Bu substituents on ligands 3 and 4 of one [M{Ln(*t*Bu<sub>2</sub>pz)<sub>4</sub>}] molecule and ligands 1 and 2 of the adjacent molecule, and lead to smaller N(12)–M–N(21) angles (85.3(1), 79.7(2) (**3La**, **Er**); 74.4(4)° (**4Sm**)).

Allocation of a formal coordination number to the alkali metal is problematic, and the previous report of a coordination number of seven for **4Er**,<sup>[24]</sup> requiring each  $\eta^3$ -*t*Bu<sub>2</sub>pz group to occupy three coordination positions, is inconsistent with  $\pi$  bonding of these groups. Formal five coordination, with each  $\eta^3$ -*t*Bu<sub>2</sub>pz effectively contributing two electron pairs, is more realistic (ignoring the possible agostic attachment of Me(133)), though most bond lengths are perhaps suggestive of a higher coordination number.

[Na(*t*Bu<sub>2</sub>pzH){Ln(*t*Bu<sub>2</sub>pz)<sub>4</sub>}]·PhMe (**5Ln**; **5Ln** = **5Nd**, **5Er**, **5Yb**): The isomorphous (triclinic, *P* $\bar{1}$ ) discrete molecular bimetallic compounds (Figure 4; Tables 7 and 8) have close structural similarities to the [Na{Ln(*t*Bu<sub>2</sub>pz)<sub>4</sub>}]<sub>n</sub> (**3La**, **3Er**) polymers. In **5Ln** a unidentate *t*Bu<sub>2</sub>pzH molecule replaces the intermolecular  $\pi$ -C(44)–Na bonds of **3Ln**, and Er–N for the same ligands of **5Er** and **3Er** are similar (Tables 7 and 5, respectively).

Binding ( $\eta^3$ -NNC) of the bridging ligands (1 and 2) to Na in **5Ln** involves unequal (0.25–0.27 Å) Na–N bonds (Table 8), similar to ligand 2 of **3Ln** (Table 6). For ligand 1, the shorter Na–N bond length is similar in **5Ln** and **3Ln**, but the longer bond length is 0.35 Å shorter in **5Ln**. With ligand 2, both Na–N distances are shorter for **5Ln**, with the difference more marked in the longer bond. One carbon of each of ligands 1 and 2 approaches Na at a bonding distance (1: 2.941(2)–3.015(3) Å; 2: 3.055(5)–3.111(2) Å) giving  $\eta^3$ -*t*Bu<sub>2</sub>pz bonding, and overall  $\mu$ - $\eta^2$ : $\eta^3$ -*t*Bu<sub>2</sub>pz ligation. The former values (Table 8) are within the range for Na–C( $\eta^4$ -

Table 7. The lanthanoid environments in [Na(*t*Bu<sub>2</sub>pzH){Ln(*t*Bu<sub>2</sub>pz)<sub>4</sub>}]·PhMe (**5Ln**; **5Ln** = **5Nd**, **5Yb**), values being listed in that order. (Data for **5Er** are accessible from the deposition).

Atom	<i>r</i>	N(12)	N(21)	N(22)	N(31)	N(32)	N(41)	N(42)
N(11)	2.465(2)	32.29(6)	84.68(6)	87.50(6)	96.67(6)	83.22(6)	165.83(7)	137.06(6)
	2.320(4)	33.8(1)	86.4(1)	89.3(1)	97.0(1)	82.9(1)	167.5(1)	136.5(1)
N(12)	2.560(2)		98.60(6)	84.43(6)	120.09(6)	94.01(6)	135.02(6)	105.20(6)
	2.449(4)		101.6(1)	86.0(1)	121.3(1)	93.5(1)	135.0(1)	103.4(1)
N(21)	2.569(2)			31.89(6)	105.65(6)	134.44(6)	93.81(6)	118.29(6)
	2.466(4)			33.3(1)	104.0(1)	134.6(1)	92.9(1)	120.3(1)
N(22)	2.486(2)				136.98(6)	164.72(6)	83.90(6)	95.19(6)
	2.345(4)				136.6(1)	166.5(1)	83.4(1)	96.5(1)
N(31)	2.420(2)					33.55(5)	97.30(6)	109.38(6)
	2.291(4)					35.0(1)	95.3(1)	107.4(1)
N(32)	2.404(2)						107.42(6)	99.88(6)
	2.287(4)						106.1(1)	96.7(1)
N(41)	2.413(2)							33.57(6)
	2.286(4)							35.5(1)
N(42)	2.408(2)							
	2.278(4)							

Table 8. Selected sodium–carbon and sodium–nitrogen distances [Å] in  $[\text{Na}(\text{tBu}_2\text{pzH})\{\text{Ln}(\text{tBu}_2\text{pz})_4\}]\cdot\text{PhMe}$  (**5Ln**; **5Ln** = **5Nd**, **5Yb**). (Data for **5Er** are available from the deposition).

Na–A, A =	<b>5Nd</b>	<b>5Yb</b>
N(11)	2.429(2)	2.411(5)
N(12)	2.665(2)	2.667(5)
N(21)	2.695(2)	2.705(5)
N(22)	2.437(2)	2.440(4)
N(51)	2.349(2)	2.353(5)
N(52) <sup>[a]</sup>	3.261(2)	3.271(5)
C(13) <sup>[a]</sup>	3.310(2)	3.280(5)
C(14) <sup>[a]</sup>	3.511(3)	3.446(6)
C(15)	3.018(3)	2.941(5)
C(23)	3.111(2)	3.053(5)
C(24) <sup>[a]</sup>	3.663(3)	3.594(5)
C(25) <sup>[a]</sup>	3.426(2)	3.389(5)

[a] "Nonbonding".

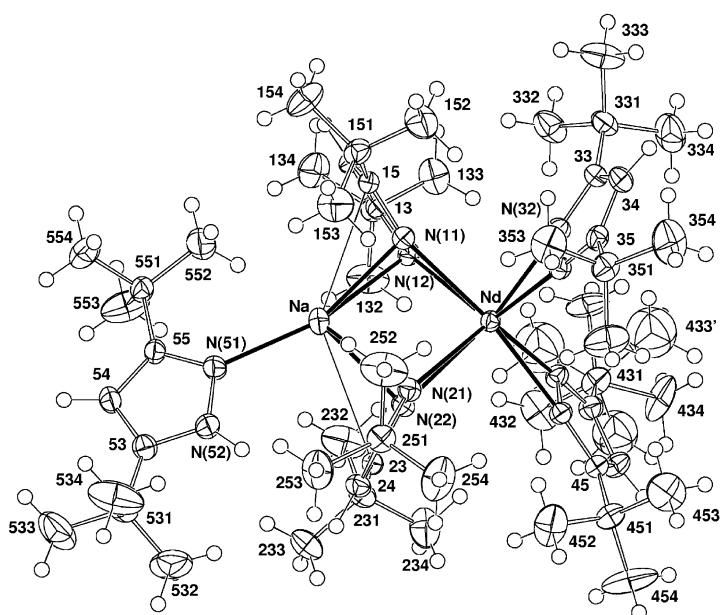


Figure 4. X-ray crystal structure of  $[\text{Na}(\eta^1\text{-tBu}_2\text{pzH})\{\text{Nd}(\text{tBu}_2\text{pz})_4\}]$  (**5Nd**), representative of **5Ln**.

PhMe) of **1Ln** (Table 2), but the latter are marginally longer (0.05–0.1 Å), though still shorter (by approximately 0.1 Å) than the additional contacts of PhMe in **1Ln**, if it is to be regarded as  $\eta^6$ -bonded. The Na–N(11 or 22)–centroid( $\text{tBu}_2\text{pz}$  ring) angles (that is, through the closest N) are 94.7–93.0 and 100.0–97.3° respectively, consistent with  $\pi$ - $\eta^3$ (NNC) bonding to Na. By contrast, the centroid( $\text{tBu}_2\text{pzH}$ )–N–Na angles of the  $\eta^1$ -pyrazole ligands are approximately 171.2–171.5°, as expected for  $\sigma$  bonding. In **5Ln**, the  $\text{tBu}$  groups of the pyrazole ligand are well separated from those of the bridging  $\text{tBu}_2\text{pz}$  ligands (Figure 4). By contrast, in **3Ln**, the  $\text{tBu}$  groups of ligands 3 and 4 of one  $[\text{Na}\{\text{Ln}(\text{tBu}_2\text{pz})_4\}]$  unit closely approach the  $\text{tBu}$  groups of ligands 1 and 2 of the adjacent unit (linked through C(44)–Na bonding) (see above).

The same coordination-number ambiguity applies for Na in **5Ln** as for Na/K in **3Ln** and **4Ln**, with five the conservative minimum.

$[\text{K}(\text{dme})\{\text{Ho}(\text{tBu}_2\text{pz})_4\}]$  (**6Ho**): Compound **6Ho** is predicted to be a monomeric bimetallic species, with a structure similar to that of class **2Ln** and a chelating DME molecule replacing an  $\eta^6$ -PhMe. The steric coordination number of DME (1.78) is smaller than that of methylcyclopentadienide (2.14) (closest analogue to toluene reported).<sup>[34b]</sup> Thus, DME can easily occupy the same coordination site as the  $\eta^6$ -toluene, that is, a face of K, and two  $\mu$ - $\eta^2$ : $\eta^5$  pyrazolate ligands can bridge Ho and K as for K/Ln in **2Ln**, with the Ho ligation completed by two terminal  $\eta^2$  pyrazolates.

## Conclusion

Elevated temperature metathesis reactions provide a convenient *general* synthesis of homoleptic  $[\text{Na}\{\text{Ln}(\text{tBu}_2\text{pz})_4\}]_n$  (**3Ln**), and  $[\text{K}\{\text{Ln}(\text{tBu}_2\text{pz})_4\}]_n$  (**4Ln**). From these a range of novel heterobimetallic complexes of the general composition  $[\text{Na}(\text{PhMe})\{\text{Ln}(\text{tBu}_2\text{pz})_4\}]$  (**1Ln**),  $[\text{K}(\text{PhMe})\{\text{Ln}(\text{tBu}_2\text{pz})_4\}]\cdot 2\text{PhMe}$  (**2Ln**) and  $[\text{Na}(\text{tBu}_2\text{pzH})\{\text{Ln}(\text{tBu}_2\text{pz})_4\}]\cdot\text{PhMe}$  (**5Ln**) have been prepared. All complexes feature  $\{\text{Ln}(\text{tBu}_2\text{pz})_4\}^-$  ions bridged to the alkali metal by two pyrazolates (**1Ln**:  $\mu$ - $\eta^2$ : $\eta^2$  +  $\mu$ - $\eta^4$ : $\eta^2$ ; **2Ln**:  $\mu$ - $\eta^2$ : $\eta^5$ ; **3,4,5Ln**:  $\mu$ - $\eta^2$ : $\eta^3$ ) with the remaining face of the alkali metal in the  $[\text{M}\{\text{Ln}(\text{tBu}_2\text{pz})_4\}]$  units covered by  $\eta^4$ -PhMe (**1Ln**),  $\eta^6$ -PhMe (**2Ln**), and  $\eta^1$ (N)-Ph<sub>2</sub>pzh (**5Ln**) ligands, or linked to another unit by  $\eta^1$ (C)-Na(K) pyrazolate coordination, giving polymeric chains (**3,4Ln**). The structures vividly illustrate the growing versatility of pyrazolate coordination. Perhaps surprisingly, the lanthanoid contraction has no effect on the structures within each series, resembling the behavior of the homoleptic  $[\text{Ln}_2(\text{tBu}_2\text{pz})_6]$  (Ln = La–Lu) series.<sup>[32]</sup> The elevated-temperature metathesis approach should prove to be of wide significance in accessing homoleptic complexes.

## Experimental Section

All products and some starting materials were air-sensitive. These required use of Schlenk and vacuum-line techniques, and therefore manipulation in an inert atmosphere. All solvents were pre-dried with sodium metal and then further dried by distillation over sodium and sodium benzophenone.  $\text{LnCl}_3$  (Ln = La, Nd, Sm, Ho, Tb) were purchased from Cerac,  $\text{ErCl}_3$  was bought from Aldrich,  $\text{NdCl}_3$  and  $\text{YbCl}_3$  were prepared by a literature method<sup>[27]</sup> and  $\text{K}(\text{tBu}_2\text{pz})$  was prepared as previously described.<sup>[55]</sup> The metal analyses were adapted from the method described in a previous paper.<sup>[39a]</sup> The Campbell Microanalytical Laboratory of the University of Otago, New Zealand, performed the microanalyses. Samples were transported sealed under nitrogen. Listed infrared data, using a Perkin Elmer 1600 FTIR spectrometer, are of Nujol mulls for the region 4000–650  $\text{cm}^{-1}$ .  $^1\text{H}$  NMR spectra were recorded with a Bruker DRX400 spectrometer. Visible/near-IR spectra were recorded with a Varian-Cary 17 spectrophotometer. Molar absorption coefficients ( $\epsilon$ ) are given in  $\text{mol dm}^{-3}\text{cm}^{-1}$ .

**Na( $\text{tBu}_2\text{pz}$ ):** Na( $\text{tBu}_2\text{pz}$ ) was synthesized by heating  $\text{tBu}_2\text{pzH}$  (2.97 g, 16.47 mmol) and NaH (0.43 g, 17.92 mmol) in toluene (40 mL) at 100–110°C for 6–8 h. The solvent was then removed under vacuum and no further purification was carried out on the remaining white product. IR:  $\tilde{\nu}$  = 1560 w, 1496 vs, 1396 m, 1360 vs, 1300 m, 1248 vs, 1208 s, 1161 m, 1134 m, 1064 m, 1016 m, 1008 s, 994 m, 782 vs, 734 m, 695  $\text{cm}^{-1}$ .

**General:** The alkali metal 3,5-di-*tert*-butylpyrazolate, the appropriate lanthanoid(III) halide (amounts below) and only for reactions utilizing  $\text{K}(\text{tBu}_2\text{pz})$ , 1,2,4,5-tetramethylbenzene (TMB), were sealed in a Carius



tube under a vacuum of  $\approx 10^{-2}$  Torr. The Carius tube was heated in an oven (conditions with individual compounds), and upon completion of the reaction, accompanied by solidification of the reaction mixture, the contents of the tube were transferred to a Schlenk flask. 1,2,4,5-Tetramethylbenzene was removed by extraction with hexane and filtration (canula). The products were then extracted by stirring with toluene and filtered. Reduction of the filtrate volume and cooling produced crystals (some of which were separated for X-ray crystallography). The bulk was filtered off under vacuum. Heating of a representative member (**3Er**, **2La**) indicates that **2Ln** and **3Ln** are thermally stable (m.p.  $>300^\circ\text{C}$ ), with loss of toluene observed at  $60^\circ\text{C}$  for **2La**. This caused the clear solid to become opaque, with no other visible change noted. Compounds **5Nd** and **5Er** lost *t*Bu<sub>2</sub>pzH at  $155^\circ\text{C}$ – $160^\circ\text{C}$  and **5Nd** melted at  $207$ – $214^\circ\text{C}$ , but **5Er** did not melt below  $360^\circ\text{C}$ . The single crystals changed slowly from clear to opaque at the surface when placed in oil for X-ray crystallography.

**Synthesis of [Na(La(*t*Bu<sub>2</sub>pz)<sub>4</sub>)]<sub>n</sub> (**3La**):** LaCl<sub>3</sub> (0.35 g, 1.43 mmol) and Na(*t*Bu<sub>2</sub>pz) (1.13 g, 5.58 mmol) were heated at  $250^\circ\text{C}$  for five days and then at  $300^\circ\text{C}$  for seven days. The white solid obtained was then extracted with toluene (60 mL) and the solvent was removed under vacuum until crystallization occurred. The mixture was placed in an ultrasonic bath overnight to redissolve the crystalline product and the solution was then cooled to  $-10^\circ\text{C}$ . Colorless crystals of **3La** were deposited and collected. Yield: 0.17 g (14%). IR:  $\tilde{\nu} = 1596$  m, 1520 s, 1503 vs, 1404 s, 1360 vs, 1304 m, 1251 vs, 1222 vs, 1203 s, 1154 m, 1103 m, 1018 s, 1007 m (sh), 983 vs, 929 w, 814 m, 793 s, 726 s, 693  $\text{cm}^{-1}$ ; <sup>1</sup>H NMR (C<sub>6</sub>D<sub>6</sub>):  $\delta = 1.24$  (s, 72H; *t*Bu), 6.11 (s, 4H; H4 pz); elemental analysis calcd (%) for C<sub>44</sub>H<sub>76</sub>LaN<sub>8</sub>Na (879.04): C 60.12, H 8.71, N 12.75, La 15.81; found: C 58.45, H 8.58, N 11.88, La 15.64.

**Attempted synthesis of [Na(PhMe)[Nd(*t*Bu<sub>2</sub>pz)<sub>4</sub>]] (**1Nd**) or [Na[Nd(*t*Bu<sub>2</sub>pz)<sub>4</sub>]]<sub>n</sub> (**3Nd**); synthesis of [Na(*t*Bu<sub>2</sub>pzH)[Nd(*t*Bu<sub>2</sub>pz)<sub>4</sub>]]-PhMe (**5Nd**):** Na(*t*Bu<sub>2</sub>pz) (1.13 g, 5.58 mmol) and NdCl<sub>3</sub> (0.35 g, 1.40 mmol) were heated at  $250^\circ\text{C}$  for six days. Extraction of the blue product with toluene (50 mL, 40 mL) gave a mixture of purple-blue and colorless crystals upon cooling. X-ray crystallography revealed the purple-blue crystals to be **5Nd**. Sufficient purple-blue crystals were handpicked for microanalysis and an IR spectrum. IR:  $\tilde{\nu} = 3341$  m, 1560 m, 1515 s, 1498 vs, 1399 s, 1358 vs, 1306 s, 1286 m, 1247 vs, 1224 s, 1204 s, 1126 m, 1053 w, 1015 s, 991 s, 800 m, 790 m, 776 m, 728 s, 722 m, 714 m, 694 m, 666  $\text{cm}^{-1}$ ; elemental analysis calcd (%) for [Nd(*t*Bu<sub>2</sub>pz)<sub>4</sub>]]<sup>1/2</sup>PhMe, C<sub>58.5</sub>H<sub>100</sub>N<sub>10</sub>NaNd (1110.74): C 63.26, H 9.07, N 12.61; elemental analysis calcd (%) for **5Nd**, C<sub>62</sub>H<sub>104</sub>N<sub>10</sub>NaNd (1156.79): C 64.37, H 9.06, N 12.11; found: C 63.07, H 7.77, N 12.60; IR of the impure colorless product, Na(*t*Bu<sub>2</sub>pz):  $\tilde{\nu} = 3278$  w, 3116 w, 1563 w, 1515 s, 1498 vs, 1399 s, 1358 vs, 1306 s, 1246 vs, 1206 s, 1129 m, 1101 w, 1053 m, 1014 vs, 997 s, 776 s, 727 s, 694  $\text{cm}^{-1}$ ; elemental analysis calcd (%) for Na(*t*Bu<sub>2</sub>pz), C<sub>11</sub>H<sub>19</sub>N<sub>2</sub>Na (202.27): C 65.30, H 9.47, N 11.37; found: C 63.37, 63.67; H 9.66, 9.90; N 12.59, 12.79.

**Synthesis of [Na(PhMe)[Tb(*t*Bu<sub>2</sub>pz)<sub>4</sub>]] (**1Tb**) and [Na[Tb(*t*Bu<sub>2</sub>pz)<sub>4</sub>]]<sub>n</sub> (**3Tb**):** TbCl<sub>3</sub> (0.44 g, 1.67 mmol) and Na(*t*Bu<sub>2</sub>pz) (1.05 g, 5.18 mmol) were heated at  $250^\circ\text{C}$  for six days. Extraction with toluene yielded colorless crystals of **1Tb** (which fluoresced green under a UV lamp), but the bulk sample analyzed as **3Tb**, 0.22 g (19%). IR:  $\tilde{\nu} = 3353$  w (trace *t*Bu<sub>2</sub>pzH impurity), 1562 w, 1503 m, 1360 s, 1307 w, 1250 vs, 1226 m, 1205 w, 1018 m, 992 m, 934 w, 782 vs, 728 m, 694 w, 660  $\text{cm}^{-1}$ ; elemental analysis calcd (%) for **3Tb**, C<sub>44</sub>H<sub>76</sub>N<sub>8</sub>NaTb (899.06): C 58.78, H 8.52, N 12.46, Tb 17.69; found: C 59.15, H 8.88, N 12.41, Tb 17.55.

**Synthesis of [Na(PhMe)[Ho(*t*Bu<sub>2</sub>pz)<sub>4</sub>]] (**1Ho**) and [Na[Ho(*t*Bu<sub>2</sub>pz)<sub>4</sub>]]<sub>n</sub> (**3Ho**):** HoCl<sub>3</sub> (0.35 g, 1.29 mmol) and Na(*t*Bu<sub>2</sub>pz) (1.13 g, 5.58 mmol) were heated at  $250^\circ\text{C}$  for three days and then at  $300^\circ\text{C}$  for a further two days. Extraction of the orange residue with toluene afforded initially pale-orange single crystals of **1Ho** (metal analysis calcd (%) for C<sub>51</sub>H<sub>84</sub>HoN<sub>8</sub>Na (997.20): Ho 15.79, found 16.54) which reverted to **3Ho** on standing. Yield: 0.23 g (18%). IR:  $\tilde{\nu} = 3235$  w (*t*Bu<sub>2</sub>pzH impurity), 1570 m, 1505 m, 1497 m, 1434 m, 1410 m, 1359 m, 1307 s, 1244 vs, 1204 s, 1184 s, 1127 s, 1016 w, 1003 m (sh), 984 s, 800 w, 777 w, 746 w, 727  $\text{cm}^{-1}$ ; visible/near IR [ $\lambda_{\text{max}}$  ( $\epsilon$ ), PhMe]: 362 (28), 419 (11), 451 (50), 470 (10), 541 (6), 647 (4), 791 (1), 1143 nm (9); elemental analysis calcd (%) for **3Ho**, C<sub>44</sub>H<sub>76</sub>HoN<sub>8</sub>Na (905.05): C 58.39, H 8.46, N 12.38; elemental analysis calcd for **1Ho**, C<sub>51</sub>H<sub>84</sub>HoN<sub>8</sub>Na (997.20): C 61.43, H 8.49, N 11.24; found: C 55.03, 55.57; H 9.27, 8.78; N 11.72, 11.92.

**Synthesis of [Na(Er(*t*Bu<sub>2</sub>pz)<sub>4</sub>)]<sub>n</sub> (**3Er**) and [Na(*t*Bu<sub>2</sub>pzH)(Er(*t*Bu<sub>2</sub>pz)<sub>4</sub>)]-PhMe (**5Er**):** Na(*t*Bu<sub>2</sub>pz) (0.95 g, 4.70 mmol) was heated with ErCl<sub>3</sub> (0.38 g, 1.39 mmol) for three days at  $250^\circ\text{C}$ . Pink crystals formed in the neck of the Carius tube, which were collected and found to be **3Er** by X-ray crystallography. The pink residue was then extracted with toluene ( $2 \times 50$  mL), giving a bulk sample of **5Er**, with some single crystals which were characterized by X-ray crystallography. Yield: 0.18 g, (16%). IR:  $\tilde{\nu} = 3352$  m, 1560 w, 1504 w, 1460 vs, 1304 s, 1302 w, 1285 w, 1250 s, 1229 s, 1205 m, 1126 m, 1013 m, 1005 m, 992 m, 793 m, 730  $\text{cm}^{-1}$ ; visible/near IR [ $\lambda_{\text{max}}$  ( $\epsilon$ ), PhMe]: 380 (77), 490 (6), 522 (42), 595 (4), 654 nm (5); elemental analysis calcd (%) for **5Er**, C<sub>64</sub>H<sub>104</sub>ErN<sub>10</sub>Na (1179.82): C 63.12, H 8.89, N 11.87, Er 14.18; found: C 59.18, 59.86; H 8.87, 8.90; N 11.24, 11.24; Er 14.02; the carbon microanalysis, performed considerably later than the metal analysis, suggests loss of toluene, though the % N does not. Elemental analysis calcd for [Na(*t*Bu<sub>2</sub>pzH)(Er(*t*Bu<sub>2</sub>pz)<sub>4</sub>)]<sub>n</sub>, C<sub>55</sub>H<sub>96</sub>ErN<sub>10</sub>Na (1087.67): C 60.73, H 8.90, N 12.88.

**Synthesis of [Na(PhMe)[Yb(*t*Bu<sub>2</sub>pz)<sub>4</sub>]] (**1Yb**), [Na[Yb(*t*Bu<sub>2</sub>pz)<sub>4</sub>]]<sub>n</sub> (**3Yb**), and [Na(*t*Bu<sub>2</sub>pzH)[Yb(*t*Bu<sub>2</sub>pz)<sub>4</sub>]]-PhMe (**5Yb**):** Heating Na(*t*Bu<sub>2</sub>pz) (1.13 g, 5.58 mmol) and YbCl<sub>3</sub> (0.41 g, 1.47 mmol) at  $250^\circ\text{C}$  for one day and at  $300^\circ\text{C}$  for two days gave some yellow and a very small amount of red solids. Extraction with toluene (40 mL) gave a colorless solution from which a few colorless single crystals deposited. These were identified by X-ray crystallography as **5Yb**, followed by **1Yb**: 0.95 g (68%). Metal analysis calcd for **1Yb**, C<sub>51</sub>H<sub>84</sub>N<sub>8</sub>NaYb (1005.31): Yb 17.21; found Yb 16.36, which reverted to **3Yb** on standing IR:  $\tilde{\nu} = 3344$  vw (trace *t*Bu<sub>2</sub>pzH impurity), 1560 m, 1506 m, 1497 m, 1411 m, 1359 s, 1250 vs, 1205 m, 1179 m, 1131 m, 1017 m, 1005 m, 989 m, 800 m, 778 m, 667  $\text{cm}^{-1}$ ; visible/near IR [ $\lambda_{\text{max}}$  ( $\epsilon$ ), PhMe]: 923 (19), 941 (12), 982 nm (30); elemental analysis calcd for **3Yb**, C<sub>44</sub>H<sub>76</sub>N<sub>8</sub>NaYb (913.16): C 57.87, H 8.39, N 12.27; found: C 57.91, H 7.88, N 11.48 (elemental analysis calcd (%) for **1Yb**, C<sub>51</sub>H<sub>84</sub>N<sub>8</sub>NaYb (1005.31): C 60.93, H 8.42, N 11.15).

**Synthesis of [K(PhMe)[La(*t*Bu<sub>2</sub>pz)<sub>4</sub>]]-2 PhMe (**2La**) and [K[La(*t*Bu<sub>2</sub>pz)<sub>4</sub>]]<sub>n</sub> (**4La**):** K(*t*Bu<sub>2</sub>pz) (1.20 g, 5.50 mmol), LaCl<sub>3</sub> (0.36 g, 1.47 mmol) and TMB (1.0 g) were heated for four days at  $250^\circ\text{C}$ . Removal of TMB with hexane, extraction by toluene (50 mL, then 40 mL) and concentration yielded colorless crystals of **2La** with the bulk product analyzing for **4La**, 0.26 g (21%). IR:  $\tilde{\nu} = 1560$  m, 1517 m, 1499 s, 1421 s, 1406 s, 1359 vs, 1306 s, 1246 vs, 1204 s, 1181 s, 1130 s, 1012 m, 993 s, 984 m, 932 m, 798 m, 782 m, 668  $\text{cm}^{-1}$ ; <sup>1</sup>H NMR (C<sub>6</sub>D<sub>6</sub>):  $\delta = 1.36$  (s, 72H; *t*Bu); 6.16 (s, 4H; H4 pz); elemental analysis calcd (%) for **4La**, C<sub>44</sub>H<sub>76</sub>KLaN<sub>8</sub> (895.14): C 59.04, H 8.56, N 12.52, La 15.52; found: C 57.71, H 8.56, N 12.52, La 15.86.

**Synthesis of [K[Nd(*t*Bu<sub>2</sub>pz)<sub>4</sub>]]<sub>n</sub> (**4Nd**):** K(*t*Bu<sub>2</sub>pz) (1.20 g, 5.50 mmol) was heated with NdCl<sub>3</sub> (0.38 g, 1.4 mmol) and TMB (1.0 g) at  $200^\circ\text{C}$  for 24 h. Extraction with toluene after removal of TMB yielded large blue crystals of **4Nd**. Yield: 0.75 g (60%), m.p.  $>360^\circ\text{C}$ . IR:  $\tilde{\nu} = 1605$  w, 1516 w, 1428 m, 1409 m, 1359 s, 1312 w, 1250 m, 1225 m, 1206 w, 1081 w, 1030 w, 1015 s, 995 s, 852 w, 796 s, 763 s, 728 vs, 694  $\text{cm}^{-1}$ ; <sup>1</sup>H NMR (200 MHz) (C<sub>6</sub>D<sub>6</sub>):  $\delta = -0.23$  (br s, 72H; *t*Bu); 18.06 (s, 4H; H4 pz); visible/near IR [ $\lambda_{\text{max}}$  ( $\epsilon$ ), PhMe]: 532 (18), 575 (72), 593 (90), 745 (9), 810 nm (9); elemental analysis calcd (%) for C<sub>44</sub>H<sub>76</sub>KN<sub>8</sub>Nd (900.48): C 58.69, H 8.51, N 12.44, Nd 16.02; found: C 58.18, H 9.15, N 12.47, Nd 15.88. A data set was collected for the crystals but the structure could not be solved.

**Synthesis of [K(PhMe)[Sm(*t*Bu<sub>2</sub>pz)<sub>4</sub>]]-2 PhMe (**2Sm**) and [K[Sm(*t*Bu<sub>2</sub>pz)<sub>4</sub>]]<sub>n</sub> (**4Sm**):** K(*t*Bu<sub>2</sub>pz) (1.20 g, 5.50 mmol) was heated with SmCl<sub>3</sub> (0.36 g, 1.40 mmol) and TMB (1.0 g) at  $200^\circ\text{C}$  for 3.5 days. Work up with toluene, as for **2La**, yielded colorless plate-shaped crystals. The crystals were found by X-ray crystallography to be **2Sm** and the bulk sample analyzed as a  $1/2$  toluene solvate of **4Sm** shortly after isolation. Yield: 0.10 g (7%). Metal analysis calcd (%) for C<sub>54.5</sub>H<sub>88</sub>KN<sub>8</sub>Sm (1044.80): Sm 14.32; found 14.39, but reverted to **4Sm** on standing. IR:  $\tilde{\nu} = 1560$  w, 1517 m, 1501 m, 1408 m, 1360 s, 1308 w, 1286 w, 1250 m, 1226 m, 1206 w, 1014 m, 994 m, 798 m, 782 m, 723  $\text{cm}^{-1}$ ; <sup>1</sup>H NMR (C<sub>6</sub>D<sub>6</sub>):  $\delta = 1.05$  (s, 72H; *t*Bu); 6.51 (s, 4H; H4 pz), visible/near IR [ $\lambda_{\text{max}}$  ( $\epsilon$ ), PhMe]: 346 (14), 376 (12), 406 (4), 1077 nm (6); elemental analysis calcd for **4Sm**, C<sub>44</sub>H<sub>76</sub>KSmN<sub>8</sub> (906.60): C 58.29, H 8.45, N 12.36; found: 57.53, 57.76; H 9.08, 8.94; N 12.61, 12.66. Some of the crystals of **2Sm** were stored under low viscosity perfluoroalkyl ether oil for several weeks and a crystal of **4Sm** was isolated from powdery material formed on desolvation.

**Synthesis of [K(PhMe){Tb(*t*Bu<sub>2</sub>pz)<sub>2</sub>]}·2PhMe (2Tb) and [K{Tb(*t*Bu<sub>2</sub>pz)<sub>2</sub>}]<sub>n</sub> (4Tb):** K(*t*Bu<sub>2</sub>pz) (1.20 g, 5.50 mmol), TbCl<sub>3</sub> (0.37 g, 1.39 mmol) and TMB (1.0 g) were heated at 300 °C for three days. Work up, as for **2La**, produced large colorless crystals of **2Tb**, which fluoresced bright green upon irradiation with a UV lamp. The bulk sample initially analyzed as a 1½ solvate of **4Tb**. Yield: 0.16 g (11%); m.p. > 360 °C. Metal analysis calcd (%) for C<sub>54.5</sub>H<sub>88</sub>KN<sub>8</sub>Tb (1053.36): Tb 15.09, found 14.94, but reverted to **4Tb** on standing. IR:  $\bar{\nu}$  = 3239 vw (*t*Bu<sub>2</sub>pzH impurity), 3114 w, 1560 w, 1517 m, 1502 vs, 1424 vs, 1408 s, 1359 vs, 1308 m, 1249 vs, 1226 vs, 1206 s, 1130 m, 1014 s, 994 vs, 798 s, 782 s, 729 m, 723 cm<sup>-1</sup>; elemental analysis calcd for **4Tb**, C<sub>44</sub>H<sub>76</sub>K<sub>2</sub>TbN<sub>8</sub> (915.16): C 57.75, H 8.37, N 12.24; found: C 57.27, 57.30; H 8.43, 8.05; N 12.29, 12.32.

**Synthesis of [K(PhMe){Ho(*t*Bu<sub>2</sub>pz)<sub>2</sub>]}·2PhMe (2Ho) [K{Ho(*t*Bu<sub>2</sub>pz)<sub>2</sub>}]<sub>n</sub> (4Ho) and [K(dme){Ho(*t*Bu<sub>2</sub>pz)<sub>2</sub>]} (6Ho):** K(*t*Bu<sub>2</sub>pz) (1.20 g, 5.50 mmol), HoCl<sub>3</sub> (0.37 g, 1.36 mmol) and TMB (1.0 g) were heated at 250 °C for three days. Work up, as for **2La**, produced pale-orange single crystals of **2Ho**. Yield: 0.26 g (16%). Metal analysis calcd (%) for C<sub>65</sub>H<sub>100</sub>HoKN<sub>8</sub> (1197.57): Ho 13.77; found 13.00, which reverted to **4Ho** on standing. IR:  $\bar{\nu}$  = 3236 m (*t*Bu<sub>2</sub>pzH impurity), 1569 m, 1504 m, 1360 m, 1307 m, 1286 m, 1278 vs, 1205 m, 1179 m, 1128 s, 1016 w, 1003 m, 992 m, 802 w, 782 w, 728 w, 668 cm<sup>-1</sup>; visible/near IR [ $\lambda_{\max}$  ( $\epsilon$ ), PhMe]: 345 (38), 362 (53), 419 (23), 451 (91), 541 (11), 640 nm (5); elemental analysis calcd for **4Ho**, C<sub>44</sub>H<sub>76</sub>HoKN<sub>8</sub> (921.17): C 57.37, H 8.32, N 12.16; found C 56.73, H 8.23, N 11.93. The toluene-insoluble residue was then extracted with DME (40 mL × 2) producing pale-orange crystals of **6Ho** after cooling of the solution. Yield: 0.21 g (15%). IR:  $\bar{\nu}$  = 3232 m (*t*Bu<sub>2</sub>pzH impurity), 1570 m, 1502 m, 1429 m, 1409 m, 1358 s, 1309 s, 1279 vs, 1204 s, 1179 m, 1129 s, 1072 m, 1038 m, 1016 m, 1003 m, 992 s, 940 w, 851 w, 804 w, 793 w, 782 w, 755 w, 727 w, 698 cm<sup>-1</sup>; visible/near IR [ $\lambda_{\max}$  ( $\epsilon$ ), PhMe]: 362 (14), 419 (10), 454 (37), 539 (6), 645 nm (4); elemental analysis calcd (%) C<sub>48</sub>H<sub>80</sub>HoKN<sub>8</sub>O<sub>2</sub> (1011.29): C 57.01, H 8.57, N 11.08; found: C 57.09, 56.86; H 8.62, 8.54; N 11.29, 11.47.

**Synthesis of [K(PhMe){Yb(*t*Bu<sub>2</sub>pz)<sub>2</sub>]}·2PhMe (2Yb) and [K{Yb(*t*Bu<sub>2</sub>pz)<sub>2</sub>}]<sub>n</sub> (4Yb):** K(*t*Bu<sub>2</sub>pz) (1.20 g, 4.50 mmol), YbCl<sub>3</sub> (0.39 g, 1.40 mmol) and TMB (1.0 g) were heated to 250 °C for three days, then at 300 °C for one day. Workup, as for **2La**, gave crystals of **2Yb** (X-ray crystallography), but the bulk sample analyzed as **4Yb**. Yield: 0.08 g (8%). IR:  $\bar{\nu}$  = 1592 w, 1503 m, 1426 m, 1411 m, 1358 s, 1309 m, 1249 s, 1228 s, 1205 m, 1228 m, 1016 m, 994 m, 982 m, 797 m, 781 m, 728 w cm<sup>-1</sup>; elemental analysis calcd (%) for **4Yb**, C<sub>44</sub>H<sub>76</sub>KN<sub>8</sub>Yb (929.27): C 56.87, H 8.24, N 12.06; found: C 56.68, 56.65; H 9.68, 9.45; N 12.18, 12.14.

**Synthesis of [K(PhMe){Lu(*t*Bu<sub>2</sub>pz)<sub>2</sub>]}·2PhMe (2Lu) and [K{Lu(*t*Bu<sub>2</sub>pz)<sub>2</sub>}]<sub>n</sub> (4Lu):** K(*t*Bu<sub>2</sub>pz) (0.60 g, 2.25 mmol) and LuCl<sub>3</sub> (0.19 g, 0.68 mmol) heated to 250 °C for three days gave, after work up as for **2La**, colorless single crystals of **2Lu** (determined by X-ray crystallography), but gave a bulk sample of **4Lu**. Yield: 0.07 g (10%). IR:  $\bar{\nu}$  = 3229 m, 1568 w, 1505 m, 1461 vs, 1359 m, 1286 m, 1250 s, 1205 m, 1178 m, 1129 m, 1013 m, 1004 m, 992 m, 799 m, 728 vs, 694 cm<sup>-1</sup>; <sup>1</sup>H NMR (C<sub>6</sub>D<sub>6</sub>):  $\delta$  = 1.02 (s, 72H, *t*Bu); 6.95 (s, 4H, H4 pz); elemental analysis calcd (%) for C<sub>44</sub>H<sub>76</sub>KLuN<sub>8</sub> (931.21): C 56.75, H 8.23, N 12.03; found: C 56.51, H 8.52, N 12.30.

**Crystal/refinement data:** Full spheres of low-temperature CCD area-detector data were measured (**1Ln**; **2La**, **Tb**; **3La**; **5Ln** Bruker AXS instrument (UWA), *T* approximately 153 K; 'empirical/multiscan absorption correction (proprietary software)) (**2Sm**, **Yb**, **Lu**; **3Er** Enraf-Nonius Kappa CCD (Monash), *T* approximately 123 K) (**4Sm** Siemens CCD (Leipzig), *T* approximately 223 K) yielding *N*<sub>t</sub>(total) reflections, these merging to *N* unique (*R*<sub>int</sub> cited), *N*<sub>o</sub> with *F* > 4 $\sigma$ (*F*) being considered 'observed' and used in the large block least-squares refinements, refining anisotropic displacement parameter forms, (*x*, *y*, *z*, *U*<sub>iso</sub>)<sub>H</sub> being constrained at estimates. All data were measured using monochromatic Mo *K* $\alpha$  radiation sources,  $\lambda$  = 0.7107 Å. Conventional residuals *R*, *R*<sub>w</sub> (weights: ( $\sigma^2(F) + 0.0004 F^2$ )<sup>-1</sup>) are cited at convergence.<sup>[56]</sup> Neutral atom complex scattering factors were employed within the Xtal 3.7 program system.<sup>[57]</sup> Pertinent results are given below and in the Tables and Figures, the latter showing 50% probability amplitude displacement envelopes for the non-hydrogen atoms, hydrogen atoms having arbitrary radii of 0.1 Å; CCDC-216779–CCDC-216791 contain the supplementary crystallographic data for this paper. These data can be obtained free of charge via

www.ccdc.cam.ac.uk/conts/retrieving.html (or from the Cambridge Crystallographic Data Centre, 12, Union Road, Cambridge CB21EZ, UK; fax: (+44) 1223-336-033; or deposit@ccdc.cam.ac.uk).

**1Ln: [Na(PhMe){Ln(*t*Bu<sub>2</sub>pz)<sub>2</sub>]} (Ln = Tb, Ho) (≡ C<sub>51</sub>H<sub>84</sub>N<sub>8</sub>NaLn)** are isomorphous, monoclinic, space group *P2*<sub>1</sub>/*c* (*C*<sub>2</sub><sup>s</sup>, no. 14), *Z* = 4 f.u. (*x*, *y*, *z*, *U*<sub>iso</sub>)<sub>H</sub> were refined for both structures.

**1Tb:** *M*<sub>r</sub> = 991.2. *a* = 11.7270(6), *b* = 19.731(1), *c* = 23.714(1) Å,  $\beta$  = 97.903(1)°, *V* = 5435 Å<sup>3</sup>.  $\rho_{\text{calcd}}$  = 1.21<sub>1</sub> g cm<sup>-3</sup>.  $\mu_{\text{Mo}}$  = 1.35 mm<sup>-1</sup>; specimen: 0.30 × 0.15 × 0.13 mm; *T*<sub>min/max</sub> = 0.72.  $2\theta_{\text{max}}$  = 75°; *N*<sub>t</sub> = 113402, *N* = 28622 (*R*<sub>int</sub> = 0.041), *N*<sub>o</sub> = 20740; *R* = 0.030, *R*<sub>w</sub> = 0.034.

**1Ho:** *M*<sub>r</sub> = 997.2. *a* = 11.6968(8), *b* = 19.727(1), *c* = 23.681(2) Å,  $\beta$  = 98.213(2)°, *V* = 5408 Å<sup>3</sup>.  $\rho_{\text{calcd}}$  = 1.22<sub>5</sub> g cm<sup>-3</sup>.  $\mu_{\text{Mo}}$  = 1.51 mm<sup>-1</sup>; specimen: 0.19 × 0.16 × 0.06 mm; *T*<sub>min/max</sub> = 0.61.  $2\theta_{\text{max}}$  = 65°; *N*<sub>t</sub> = 112241, *N* = 19123 (*R*<sub>int</sub> = 0.078), *N*<sub>o</sub> = 13409; *R* = 0.033, *R*<sub>w</sub> = 0.034.

**2Ln: [K(PhMe){Ln(*t*Bu<sub>2</sub>pz)<sub>2</sub>]}·2PhMe (Ln = La, Sm, Tb, Yb, Lu) (≡ C<sub>65</sub>H<sub>100</sub>KN<sub>8</sub>Ln)** are isomorphous, orthorhombic, space group *Prma* (*D*<sub>2</sub><sup>16</sup>, No. 62, *Z* = 4 f.u. As modelled in this space group, Ln, K, C(151,231,103,203,206) lie in the crystallographic mirror plane *y* = 0.25, associated pertinent ligand components disordered to either side, site occupancies obligate 0.5. *t*Butyl substituent 33 was modeled as rotationally disordered about the pendant bond, site occupancies set at 0.5.

**2La:** *M*<sub>r</sub> = 1171.6. *a* = 23.208(3), *b* = 17.878(3), *c* = 16.190(2) Å, *V* = 6717 Å<sup>3</sup>.  $\rho_{\text{calcd}}$  = 1.15<sub>8</sub> g cm<sup>-3</sup>.  $\mu_{\text{Mo}}$  = 0.74 mm<sup>-1</sup>; specimen: 0.32 × 0.30 × 0.18 mm; *T*<sub>min/max</sub> = 0.58.  $2\theta_{\text{max}}$  = 58°; *N*<sub>t</sub> = 65382, *N* = 8936 (*R*<sub>int</sub> = 0.082), *N*<sub>o</sub> = 4451; *R* = 0.063, *R*<sub>w</sub> = 0.074.

**2Sm:** *M*<sub>r</sub> = 1183.0. *a* = 23.161(5), *b* = 17.715(4), *c* = 16.227(3) Å, *V* = 6658 Å<sup>3</sup>.  $\rho_{\text{calcd}}$  = 1.18<sub>0</sub> g cm<sup>-3</sup>.  $\mu_{\text{Mo}}$  = 0.99 mm<sup>-1</sup>; specimen: not recorded (no correction).  $2\theta_{\text{max}}$  = 53°; *N*<sub>t</sub> = 62214, *N* = 7026 (*R*<sub>int</sub> = 0.094), *N*<sub>o</sub> = 4756; *R* = 0.055, *R*<sub>w</sub> = 0.10.

**2Tb:** *M*<sub>r</sub> = 1191.6. *a* = 23.138(2), *b* = 17.657(2), *c* = 16.203(1) Å, *V* = 6620 Å<sup>3</sup>.  $\rho_{\text{calcd}}$  = 1.19<sub>5</sub> g cm<sup>-3</sup>.  $\mu_{\text{Mo}}$  = 1.17 mm<sup>-1</sup>; specimen: 0.24 × 0.18 × 0.06 mm; *T*<sub>min/max</sub> = 0.70.  $2\theta_{\text{max}}$  = 58°; *N*<sub>t</sub> = 136131, *N* = 9076 (*R*<sub>int</sub> = 0.085), *N*<sub>o</sub> = 6152; *R* = 0.056, *R*<sub>w</sub> = 0.087.

**2Yb:** *M*<sub>r</sub> = 1205.7. *a* = 23.099(5), *b* = 17.536(3), *c* = 16.232(3) Å, *V* = 6575 Å<sup>3</sup>.  $\rho_{\text{calcd}}$  = 1.21<sub>8</sub> g cm<sup>-3</sup>.  $\mu_{\text{Mo}}$  = 1.53 mm<sup>-1</sup>; specimen: not recorded (no correction).  $2\theta_{\text{max}}$  = 53°; *N*<sub>t</sub> = 43709, *N* = 6879 (*R*<sub>int</sub> = 0.011), *N*<sub>o</sub> = 3999; *R* = 0.059, *R*<sub>w</sub> = 0.094.

**2Lu:** *M*<sub>r</sub> = 1207.6. *a* = 23.091(5), *b* = 17.516(4), *c* = 16.236(3) Å, *V* = 6569 Å<sup>3</sup>.  $\rho_{\text{calcd}}$  = 1.22<sub>1</sub> g cm<sup>-3</sup>.  $\mu_{\text{Mo}}$  = 1.61 mm<sup>-1</sup>; specimen: not recorded (no correction).  $2\theta_{\text{max}}$  = 53°; *N*<sub>t</sub> = 68950, *N* = 6874 (*R*<sub>int</sub> = 0.083), *N*<sub>o</sub> = 4821; *R* = 0.065, *R*<sub>w</sub> = 0.013.

**3Ln, 4Ln: [Na(Ln(*t*Bu<sub>2</sub>pz)<sub>2</sub>)]<sub>(n=2)</sub> (Ln = La, Er; 3Ln); [K(Ln(*t*Bu<sub>2</sub>pz)<sub>2</sub>)]<sub>(n=2)</sub> (Ln = Sm; 4Sm) (≡ C<sub>44</sub>H<sub>76</sub>N<sub>8</sub>(Na/K)Ln)** are isomorphous, monoclinic, space group *P2*<sub>1</sub>/*m* (*C*<sub>2</sub><sup>i</sup>, No.10, *Z* = 2 f.u. The polymer lies about a mirror plane (*y* = 0.25), Ln, Na/K, C(132, 34, 44) lying in the plane with disorder of the remainder of the associated ligands to either side, occupancies obligate 0.5.

**3La:** *M*<sub>r</sub> = 879.0. *a* = 9.651(1), *b* = 20.449(3), *c* = 12.564(2) Å,  $\beta$  = 102.842(3)°, *V* = 2418 Å<sup>3</sup>.  $\rho_{\text{calcd}}$  = 1.20<sub>7</sub> g cm<sup>-3</sup>.  $\mu_{\text{Mo}}$  = 0.93 mm<sup>-1</sup>; specimen: 0.30 × 0.25 × 0.20 mm; *T*<sub>min/max</sub> = 0.84.  $2\theta_{\text{max}}$  = 70°; *N*<sub>t</sub> = 43888, *N* = 10931 (*R*<sub>int</sub> = 0.036), *N*<sub>o</sub> = 9059; *R* = 0.045, *R*<sub>w</sub> = 0.053.

**3Er:** *M*<sub>r</sub> = 907.4. *a* = 9.614(2), *b* = 20.424(4), *c* = 12.302(3) Å,  $\beta$  = 102.50(3)°, *V* = 2358 Å<sup>3</sup>.  $\rho_{\text{calcd}}$  = 1.27<sub>8</sub> g cm<sup>-3</sup>.  $\mu_{\text{Mo}}$  = 1.83 mm<sup>-1</sup>; specimen: 0.30 × 0.25 × 0.17 mm; (no correction).  $2\theta_{\text{max}}$  = 57°; *N*<sub>t</sub> = 26975, *N* = 6007 (*R*<sub>int</sub> = 0.040), *N*<sub>o</sub> = 5085; *R* = 0.035, *R*<sub>w</sub> = 0.043.

**4Sm:** *M*<sub>r</sub> = 906.6. *a* = 9.946(2), *b* = 20.517(4), *c* = 12.639(3) Å,  $\beta$  = 103.04(3)°, *V* = 2513 Å<sup>3</sup>.  $\rho_{\text{calcd}}$  = 1.19<sub>8</sub> g cm<sup>-3</sup>.  $\mu_{\text{Mo}}$  = 1.29 mm<sup>-1</sup>; specimen: 0.30 × 0.25 × 0.17 mm; *T*<sub>min/max</sub> = 0.44.  $2\theta_{\text{max}}$  = 53°; *N*<sub>t</sub> = 13990, *N* = 5263 (*R*<sub>int</sub> = 0.072), *N*<sub>o</sub> = 3615; *R* = 0.072, *R*<sub>w</sub> = 0.085.

**5Ln: [Na(*t*Bu<sub>2</sub>pzH){Ln(*t*Bu<sub>2</sub>pz)<sub>2</sub>]}·PhMe (Ln = Nd, Er, Yb) (≡ C<sub>62</sub>H<sub>104</sub>N<sub>10</sub>NaLn)** are isomorphous, triclinic, space group *P* $\bar{1}$  (*C*<sub>1</sub><sup>i</sup>, no. 2, *Z* = 2. *tert*-Butyl 24 was modeled as rotationally disordered about the pendant bond over two sets of sites for Ln = Nd, Er, occupancies set at 0.5 after trial refinement for Ln = Nd, 0.782(4) and complement for Ln = Er, and fully ordered for Ln = Yb.

**5Nd:** *M*<sub>r</sub> = 1156.8. *a* = 13.2558(8), *b* = 15.3232(9), *c* = 16.3948(10) Å,  $\alpha$  = 88.260(2),  $\beta$  = 82.988(2),  $\gamma$  = 87.695(2)°, *V* = 3302 Å<sup>3</sup>.  $\rho_{\text{calcd}}$  = 1.16<sub>1</sub> g cm<sup>-3</sup>.  $\mu_{\text{Mo}}$  = 0.84 mm<sup>-1</sup>; specimen: 0.18 × 0.10 × 0.06 mm; *T*<sub>min/max</sub> = 0.89.  $2\theta_{\text{max}}$  =

75°;  $N_1=61\,142$ ,  $N=28\,902$  ( $R_{\text{int}}=0.043$ ),  $N_o=19\,612$ ;  $R=0.045$ ,  $R_w=0.038$ .

**5Er**:  $M_r=1179.8$ .  $a=13.2105(7)$ ,  $b=15.3022(8)$ ,  $c=16.2484(9)$  Å,  $\alpha=88.632(1)$ ,  $\beta=82.847(1)$ ,  $\gamma=87.985(1)^\circ$ ,  $V=3256$  Å<sup>3</sup>.  $\rho_{\text{calc}}=1.20_3$  g cm<sup>-3</sup>.  $\mu_{\text{Mo}}=1.34$  mm<sup>-1</sup>; specimen:  $0.32 \times 0.21 \times 0.18$  mm;  $T_{\text{min/max}}=0.83$ .  $2\theta_{\text{max}}=75^\circ$ ;  $N_1=66\,682$ ,  $N=33\,392$  ( $R_{\text{int}}=0.029$ ),  $N_o=27\,570$ ;  $R=0.031$ ,  $R_w=0.027$ . ( $x$ ,  $y$ ,  $z$ ,  $U_{\text{iso}}$ )<sub>H</sub> were refined throughout (minor component of *t*Butyl 24 excepted).

**5Yb**:  $M_r=1185.6$ .  $a=13.208(1)$ ,  $b=15.281(1)$ ,  $c=16.199(1)$  Å,  $\alpha=88.791(2)$ ,  $\beta=82.726(2)$ ,  $\gamma=88.098(2)^\circ$ ,  $V=3241$  Å<sup>3</sup>.  $\rho_{\text{calc}}=1.21_3$  g cm<sup>-3</sup>.  $\mu_{\text{Mo}}=1.49$  mm<sup>-1</sup>; specimen:  $0.25 \times 0.21 \times 0.16$  mm;  $T_{\text{min/max}}=0.90$ .  $2\theta_{\text{max}}=58^\circ$ ;  $N_1=67\,615$ ,  $N=17\,051$  ( $R_{\text{int}}=0.056$ ),  $N_o=14\,228$ ;  $R=0.051$ ,  $R_w=0.073$ .

## Acknowledgement

We are grateful to Jens Baldamus for collection of crystallographic data for **4Sm**. We also acknowledge financial support of the Australian Research Council and an Australian Post Graduate Award for R.H.

- [1] F. T. Edelmann "Scandium, Yttrium, Lanthanides and Actinides, and Titanium Group" (Ed.: M. F. Lappert) in *Comprehensive Organometallic Chemistry II*, Pergamon, Oxford **1995**, Vol. 4, p. 11.
- [2] M. N. Bochkarev, L. N. Zakharov, G. S. Kalinina, *Organoderivatives of Rare Earth Elements*, Kluwer, Dordrecht, **1995**.
- [3] R. Anwander, *Top. Organomet. Chem.* **1999**, 2, 1–61.
- [4] F. T. Edelmann, D. M. M. Freckmann, H. Schumann, *Chem. Rev.* **2002**, 102, 1851–1896.
- [5] a) R. Kempe, *Angew. Chem. Int. Ed.* **2000**, 39, 468–493; *Angew. Chem.* **2000**, 112, 478–504; b) R. Kempe, H. Noss, T. Irrgang, *J. Organomet. Chem.* **2002**, 647, 12–20.
- [6] a) R. Anwander, *Top. Curr. Chem.* **1996**, 179, 33–112; b) F. T. Edelmann, *Coord. Chem. Rev.* **1994**, 137, 403–481.
- [7] G. B. Deacon, C. M. Forsyth in *Inorganic Chemistry Highlights* (Eds.: G. Meyer, D. Naumann, L. Wesemann), Wiley-VCH, Weinheim, **2002**, Chapter 7, pp. 139–153.
- [8] *Alkoxo and Aryloxo Derivatives of Metals* (Eds.: D. C. Bradley, R. C. Mehrota, I. Rothwell, A. Singh), Academic Press, London, **2001**.
- [9] a) L. G. Hubert-Pfalzgraf, *New J. Chem.* **1995**, 19, 727–750; L. G. Hubert-Pfalzgraf, *Coord. Chem. Rev.* **1998**, 178–180, 967–997; b) W. J. Evans, *New J. Chem.* **1995**, 19, 525–533.
- [10] a) D. C. Bradley, J. S. Ghotra, F. A. Hart, *J. Chem. Soc. Chem. Commun.* **1972**, 349–350; D. C. Bradley, J. S. Ghotra, F. A. Hart, *J. Chem. Soc. Dalton Trans.* **1973**, 1021–1023; b) E. C. Alyea, D. C. Bradley, R. G. Copperwaithe, *J. Chem. Soc. Dalton Trans.* **1972**, 1580–1584; c) J. S. Ghotra, M. B. Hursthouse, A. J. Welch, *J. Chem. Soc. Chem. Commun.* **1973**, 669–670.
- [11] P. B. Hitchcock, M. F. Lappert, A. Singh, *J. Chem. Soc. Chem. Commun.* **1983**, 1499–1501.
- [12] a) C. Eaborn, P. B. Hitchcock, K. Izod, J. D. Smith, *J. Am. Chem. Soc.* **1994**, 116, 12071–12072; b) C. Eaborn, P. B. Hitchcock, K. Izod, J. D. Smith, Z.-R. Lu, *Organometallics* **1996**, 15, 4783–4790.
- [13] a) J. R. van den Hende, P. B. Hitchcock, M. F. Lappert, *J. Chem. Soc. Chem. Commun.* **1994**, 1413–1414; b) J. R. van den Hende, P. B. Hitchcock, S. Holmes, M. F. Lappert, *J. Chem. Soc. Dalton Trans.* **1995**, 1435–1439.
- [14] G. B. Deacon, C. M. Forsyth, P. C. Junk, B. W. Skelton, A. H. White, *Chem. Eur. J.* **1999**, 5, 1452–1459.
- [15] P. B. Hitchcock, M. F. Lappert, R. G. Smith, R. A. Bartlett, P. P. Power, *J. Chem. Soc. Chem. Commun.* **1988**, 1007–1009.
- [16] G. B. Deacon, T. Feng, C. M. Forsyth, A. Gitlits, D. C. Hockless, Q. Shen, B. W. Skelton, A. H. White, *J. Chem. Soc. Dalton Trans.* **2000**, 961–966.
- [17] D. L. Clark, J. C. Gordon, J. C. Huffman, *Inorg. Chem.* **1992**, 31, 1554–1556.
- [18] D. L. Clark, J. C. Gordon, J. C. Huffman, R. V. Hollis, J. G. Watkin, B. D. Zwick, *Inorg. Chem.* **1994**, 33, 5903–5911.
- [19] D. L. Clark, R. V. Hollis, B. L. Scott, J. G. Watkin, *Inorg. Chem.* **1996**, 35, 667–674.
- [20] D. L. Clark, G. B. Deacon, T. Feng, R. L. Vincent-Hollis, B. L. Scott, B. W. Skelton, J. G. Watkin, A. H. White, *J. Chem. Soc. Chem. Commun.* **1996**, 1729–1730.
- [21] G. B. Deacon, T. Feng, P. C. Junk, B. W. Skelton, A. H. White, *J. Chem. Soc. Dalton Trans.* **1997**, 1181–1186.
- [22] L.-L. Zhang, Y.-M. Yao, Y.-J. Luo, Q. Shen, *Polyhedron* **2000**, 19, 2243–2247.
- [23] a) J. E. Cosgriff, G. B. Deacon, *Angew. Chem.* **1998**, 110, 298–299; *Angew. Chem. Int. Ed.* **1998**, 37, 286–287; b) F. Nief, *Eur. J. Inorg. Chem.* **2001**, 891–904; c) D. Pfeiffer, B. J. Ximba, L. M. Liable-Sands, A. L. Rheingold, M. J. Heeg, D. M. Coleman, H. B. Schlegel, T. F. Kuech, C. H. Winter, *Inorg. Chem.* **1999**, 38, 4539–4548; d) G. B. Deacon, C. M. Forsyth, A. Gitlits, R. Harika, P. C. Junk, B. W. Skelton, A. H. White, *Angew. Chem.* **2002**, 114, 3383–3385; *Angew. Chem. Int. Ed.* **2002**, 41, 3249–3251;
- [24] G. B. Deacon, E. E. Delbridge, C. M. Forsyth, *Angew. Chem.* **1999**, 111, 1880–1882; *Angew. Chem. Int. Ed.* **1999**, 38, 1766–1767.
- [25] a) J. E. Cosgriff, G. B. Deacon, B. M. Gatehouse, H. Hemling, H. Schumann, *Aust. J. Chem.* **1994**, 47, 1223–1235; b) J. E. Cosgriff, G. B. Deacon, G. D. Fallon, B. M. Gatehouse, H. Schumann, R. Weimann, *Chem. Ber.* **1996**, 129, 953–958.
- [26] a) L. R. Falvello, J. Fornies, A. Martin, R. Navarro, V. Sicilia, P. Villarroya, *Chem. Commun.* **1998**, 2429–2430; b) J. R. Perera, M. J. Heeg, H. B. Schlegel, C. H. Winter, *J. Am. Chem. Soc.* **1999**, 121, 4536–4537; c) K. Most, S. Köpke, F. Dall Antonia, N. C. Mösch-Zanetti, *Chem. Commun.* **2002**, 1676–1677; d) J. Röder, F. Meyer, E. Kaifer, *Angew. Chem.* **2002**, 114, 2414–2416; *Angew. Chem. Int. Ed.* **2002**, 41, 2304–2306; e) T. Beringhelli, G. D'Alfonso, M. Panigati, P. Mercandelli, A. Sironi, *Chem. Eur. J.* **2002**, 8, 5340–5350; f) A. Steiner, G. T. Lawson, B. Walford, D. Leusser, D. Stalke, *J. Chem. Soc. Dalton Trans.* **2001**, 219–221.
- [27] *Synthesis of Lanthanoid and Actinide Compounds* (Eds.: G. Meyer, L. R. Morss), Kluwer, Boston, **1991**; (Topics in f-Element Chemistry, Vol. 2).
- [28] G. B. Deacon, R. Harika, P. C. Junk, A. H. White, B. W. Skelton, unpublished results.
- [29] a) D. C. Stewart, D. Kato, *Anal. Chem.* **1958**, 30, 164–172; b) C. H. Evans, *Biochemistry of the Lanthanoids*, Plenum, New York, **1990**.
- [30] G. B. Deacon, A. G. Gitlits, B. W. Skelton, A. H. White, *Chem. Commun.* **1999**, 1213–1214.
- [31] G. B. Deacon, E. E. Delbridge, B. W. Skelton, A. H. White, *Eur. J. Inorg. Chem.* **1998**, 543–545.
- [32] G. B. Deacon, A. Gitlits, P. W. Roesky, M. R. Burgstein, K. C. Lim, B. W. Skelton, A. H. White, *Chem. Eur. J.* **2001**, 7, 127–138.
- [33] R. D. Shannon, *Acta Crystallogr. Sect. A* **1976**, 32, 751–767.
- [34] a) C. T. Abrahams, PhD Thesis, Monash University, **1996**; b) J. Marçalo, P. de Matos, *Polyhedron* **1989**, 8, 2431–2437.
- [35] M. Johnson, J. C. Taylor, G. W. Cox, *J. Appl. Crystallogr.* **1980**, 13, 188–189.
- [36] I. A. Guzei, G. P. A. Yap, A. H. Rheingold, H. B. Schlegel, C. H. Winter, *J. Am. Chem. Soc.* **1997**, 119, 3387–3388.
- [37] C. Yelamos, M. J. Heeg, C. H. Winter, *Inorg. Chem.* **1999**, 38, 1871–1878.
- [38] J. E. Cosgriff, G. B. Deacon, B. M. Gatehouse, H. Hemling, H. Schumann, *Angew. Chem.* **1993**, 105, 906–907; *Angew. Chem. Int. Ed. Engl.* **1993**, 32, 874–875.
- [39] a) J. E. Cosgriff, G. B. Deacon, B. M. Gatehouse, *Aust. J. Chem.* **1993**, 46, 1881–1896; b) J. E. Cosgriff, G. B. Deacon, B. M. Gatehouse, P. R. Lee, H. Schumann, *Z. Anorg. Allg. Chem.* **1996**, 622, 1399–1403.
- [40] K. W. Klinkhammer, *Chem. Eur. J.* **1997**, 3, 1418–1431.
- [41] R. Wochele, W. Schwarz, K. W. Klinkhammer, K. Locke, J. Weidlein, *Z. Anorg. Allg. Chem.* **2000**, 626, 1963–1973 (Distances (from CCDC refcode FOZWOG) are not mentioned in the original publication).
- [42] S. Chadwick, U. Englich, K. Ruhlandt-Senge, *Organometallics* **1997**, 16, 5792–5803.

- [43] L. Rösch, G. Altnan, C. Krüger, Y.-H. Tsay, *Z. Naturforsch* **1983**, *38b*, 34–41.
- [44] C. J. Schaverien, J. B. van Mechelen, *Organometallics* **1991**, *10*, 1704–1709 (Distances (from CCDC refcode KIXNEK) are not in the original publication).
- [45] E. Leiner, O. Hampe, M. Scheer, *Eur. J. Inorg. Chem* **2002**, 584–590.
- [46] M. A. Beswick, N. Choi, A. D. Hopkins, M. McPartlin, *Chem. Commun.* **1998**, 261–262.
- [47] P. B. Hitchcock, M. F. Lappert, A. V. Protchenko, *J. Am. Chem. Soc.* **2001**, *123*, 189–190.
- [48] P. B. Hitchcock, M. F. Lappert, G. A. Lawless, B. Royo, *J. Chem. Soc. Chem. Commun.* **1993**, 554–555.
- [49] C. Kayser, R. D. Fischer, J. Baumgartner, C. Marschner, *Organometallics* **2002**, *21*, 1023–1030.
- [50] D. A. Hoic, M. Di Mare, G. C. Fu, *J. Am. Chem. Soc.* **1997**, *119*, 7155–7156.
- [51] M. Unverzagt, H.-J. Winkler, M. Brock, M. Hofmann, P. von R. Schleyer, W. Massa, A. Berndt, *Angew. Chem. Int. Ed. Engl.* **1997**, *36*, 853–855; *Angew. Chem.* **1997**, *109*, 879–882.
- [52] W. Zheng, N. C. Mösch-Zanetti, T. Blunck, H. W. Roesky, M. Noltemeyer, H.-G. Schmidt, *Organometallics* **2001**, *20*, 3299–3303.
- [53] W. Zheng, M. J. Heeg, C. H. Winter, *Angew. Chem.* **2003**, *115*, 2867–2870; *Angew. Chem. Int. Ed.* **2003**, *42*, 2761–2764.
- [54] N. C. Mösch-Zanetti, M. Ferbinteanu, J. Magull, *Eur. J. Inorg. Chem.* **2002**, 950–956.
- [55] C. Yelamos, M. J. Heeg, C. H. Winter, *Inorg. Chem.* **1998**, *37*, 3892–3894.
- [56] Final refinements on all structures were carried out at The University of Western Australia.
- [57] S. R. Hall, D. J. du Boulay, R. Olthof-Hazekamp (eds.), *The Xtal 3.7 System*, University of Western Australia, 2001.

Received: August 13, 2003

Revised: September 2, 2003 [F5444]